Dynamical theory for strongly correlated two-dimensional electron systems

D. Neilson and L. Świerkowski*
School of Physics, University of New South Wales, Kensington 2033, Sydney, Australia

A. Sjölander
Institute for Theoretical Physics, Chalmers Technical University, S412 96 Göteborg, Sweden

J. Szymański
Telecom Australia Research Laboratories, 770 Blackburn Road, Clayton 3168, Melbourne, Australia
(Received 2 January 1991; revised manuscript received 16 April 1991)

We describe a method for treating the time-dependent behavior of the electron cloud surrounding each electron in a two-dimensional electron gas. The method is based on a conserving solution of the quantum kinetic equation for the relaxation function of the system using the Mori formalism with two distinct memory functions, one for the collective degrees of freedom and one for the single-particle modes. At lower electron densities these dynamic effects are shown to become increasingly important and to play a part in the eventual solidification into a Wigner crystal. We find that the plasmon resonance energy $\omega_p(\mathbf{q})$ is strongly depressed compared with the random-phase approximation, leading to a negative dispersion for large $\mathbf{q}$ in the low-density region. We have determined the width of the plasmon peak and find that as the Wigner-crystal transition point is approached, the plasmon peak remains well defined even for $\mathbf{q}$ comparable to the Fermi momentum. For $r_s \gtrsim 20$, we observe a low-energy peak in the excitation spectrum of the electron liquid for values of $\mathbf{q}$ matching the reciprocal vector of the Wigner lattice. The occurrence of this peak is matched by the appearance of a large peak in the static susceptibility at that $\mathbf{q}$ value.

I. INTRODUCTION

In the study of the interacting electron liquid the introduction of a local mean field surrounding each electron has proved to be a very useful concept. In this paper we investigate the dynamics of the interaction between an electron and its exchange-correlation hole, presenting results for a strongly correlated two-dimensional electron layer.

Hubbard[1] first introduced the idea of a static exchange hole to deal with the exchange corrections to the linear-response random-phase-approximation (RPA) perturbation expansion. The "hole" is a region of depleted electron density resulting from the antisymmetrization of the many-body electron wave function. The idea has been developed so that it now encompasses the depletion of density due to the Coulomb repulsion between electrons.[2]

The static local-field corrections are usually included by inserting a static local-field factor $G(\mathbf{q})$ into the RPA expression for the total density-density (retarded) response function of the system $\chi(\mathbf{q},\omega)$,

$$\chi(\mathbf{q},\omega) = \frac{\chi^0(\mathbf{q},\omega)}{1+[1-G(\mathbf{q})]v_{\mathbf{q}}\chi^0(\mathbf{q},\omega)} \tag{1}$$

where $\chi^0(\mathbf{q},\omega)$ is the response function of noninteracting electrons[3] (Lindhard function).

For the three-dimensional electron gas at metallic densities $G(\mathbf{q})$ is found to be a smooth function lying in the range $0 \le G(\mathbf{q}) \le 1$. For $|\mathbf{q}| \gtrsim k_F$, $G(\mathbf{q})$ approaches unity from below. Values of $G(\mathbf{q})$ lying between zero and one reflect the depletion of density around each electron in real space.

Different approaches to the calculation of the static local field $G(\mathbf{q})$ are possible. Singwi, Tosi, Land, and Sjölander[4] (STLS) developed a self-consistent scheme based on the approximate solution of the equation of motion for one-particle distribution function. Lowy and Brown[5] and Bedell and Brown[6] calculated $G(\mathbf{q})$ directly from the two-body effective interaction (t matrix) obtained from the infinite ladder sum of static Coulomb interactions between the pair of electrons. Monte Carlo numerical simulations by Ceperley and Alder[7] of the ground-state properties of the electron gas subsequently confirmed the accuracy of the pair-correlation function calculated by both STLS and Lowy and Brown for metallic densities.

A key assumption of the static exchange-correlation hole model is that the depleted surroundings around a particular electron are assumed to rigidly follow the electron as it propagates through the system and undergoes various scattering processes. In this picture the electron remains precisely at the center of its own correlation hole at all times. This should be a good approximation at high densities, $r_s \lesssim 1$, since whenever the particular electron changes its motion the time scale for the relaxation of the surrounding cloud of electrons to the new electron position is of the order of the inverse plasmon frequency ω_p^{-1}, and at high densities this is very fast.

However, at lower densities these assumptions should

become less valid. Goodman and Sjölander[8] investigated the short-time relative movement of the correlation hole and its electron. They found that even at metallic densities the transient properties of this motion significantly affect the third-moment sum rule. Iwamoto, Krotscheck, and Pines[9] used the third-moment sum rule as a way of getting information about the frequency dependence of the local-field factor and found that the dependence of $G(\mathbf{q})$ as a function of $\mathbf{q}$ was completely different in the small- and large-ω regions.

Green, Neilson, and Szymański[10] (GNS) and Green, Neilson, Pines, and Szymański[11] investigated the dynamics of the electron system by developing a systematic perturbative expansion of the most significant corrections to the RPA dynamic response function, including local-field effects. The dynamics were expressed as a sequence of independent binary collisions, and this was shown to be a good approximation for the higher metallic densities, $r_s \lesssim 4$. This would be analogous to the way one treats weakly interacting classical plasmas.

However, independent binary collisions cannot carry certain information which is crucial when considering strongly correlated systems. The situation would in certain respects resemble that faced in dense classical plasmas. In the formalism applied here, we picture the individual electrons coupled to a fluid of surrounding electrons which exhibit strong collective behavior and which can react back on the primary electron. A mean-field approximation with a static local-field correction enters as the first approximation and incorporates the static exchange-correlation hole which follows its electron rigidly. In the next approximation the dynamics of the exchange-correlation hole is included. This takes into account the nonrigid coupling between the electron and its surrounding hole. One can also view the approach as a natural extension of the GNS approach since for the higher electron densities they give essentially the same results.

By coupling the electron to density fluctuations rather than to individual random electron fluctuations, we emulate the forces associated with the dynamic density profile surrounding each electron. Density fluctuations involve the collective motion of large numbers of particles, and their time evolution can be significantly affected by overall conservation requirements such as the continuity equation. If the time evolution becomes significantly slower than the single-electron scattering time, then the density excitations may not be able to readjust sufficiently quickly to changes in the electron motion. In this case they can exert a significant force on the propagating electron, thus affecting its subsequent motion.

Using the Mori formalism[12] for treating the dynamics of many-body systems, we set up a formally exact equation for the relaxation function $R_{\mathbf{kk}'}(\mathbf{r},t)$, which introduces a memory function $M_{\mathbf{kk}'}(\mathbf{r},t)$. We show how to approximate in a conserving manner the dynamic part of this matrix by two scalar memory functions $\gamma(\mathbf{r},t)$ and $\gamma^s(\mathbf{r},t)$. The function $\gamma(\mathbf{r},t)$ gives the dynamic coupling of a density fluctuation to the surrounding exchange-correlation hole and $\gamma^s(\mathbf{r},t)$ is the corresponding function for the "single-particle" part of the density fluctuation. The introduction of $\gamma^s(\mathbf{r},t)$ makes this approach quite different from a straightforward introduction of a dynamic local field.

Our formalism has been developed in analogy to the successful approach to classical liquids and plasmas based on the classical notion of self-motion.[13] The extension of the Mori formalism to quantum fluids, particularly with liquid helium in mind, was done by Boley and Smith[14] and by Valls and co-workers[15] and they discussed at length the formal aspects of such a theory. Götze[16] has in a series of papers applied the Mori formalism to the localization problem of electrons in disordered systems. A controversy arose with this work concerning the treatment of interference effects. We believe that neither interference effects nor exchange effects play any crucial role in Wigner crystallization, but that the dominant role is played by the ordinary spatial correlations between electrons. The main objection to Götze's work in this regard should therefore not be relevant here. Wigner crystallization is known to occur both in classical and quantum plasmas, and we believe it is dominated by classical effects.

Since correlations play a more important role for the two-dimensional (2D) system than for the three-dimensional one, and since there is a much higher experimental possibility for the two-dimensional system of lowering the electron density down to the Wigner crystal regime, we concentrate here on the two-dimensional case. From computer simulations for the ground state of the uniform 2D electron system we know that Wigner crystallization should occur for a density around $r_s \simeq 40$. We are therefore mainly concerned with what happens at these very low densities before crystallization occurs. However, our treatment does not include the phase transition itself.

Section II introduces the microscopic memory function for quantum systems and describes how we approximate it. The appendixes contain some details of the memory function formalism which we have applied to this dynamical problem. Our approach can be applied in the strongly correlated region of the electron liquid, $5 \lesssim r_s \lesssim 40$. In Sec. III we present results in this range of densities for the plasmon dispersion $\omega_p(\mathbf{q})$, the width of the plasmon peak, and the retarded density-density response function $\chi(\mathbf{q},\omega)$. Section IV contains concluding remarks.

II. KINETIC EQUATIONS

In this section we set up our equations of motion which incorporate the effects of the dynamic interaction between excitations and their surroundings. The surroundings react back on the excitations through the time-dependent memory function. The effect of the excitations themselves is contained in the generalized (retarded) response function $\chi_{\mathbf{kk}'}(\mathbf{q},t)$.

The function $\chi_{\mathbf{kk}'}(\mathbf{q},t)$ gives the response of one of the system's microscopic degrees of freedom, labeled $\mathbf{k}$, to an external stimulus of wavelength $\mathbf{q}$ which couples only to the $\mathbf{k}'$ degree of freedom. It is related to the density-density response function $\chi(\mathbf{q},t)$ by a summation over $\mathbf{k}$ and $\mathbf{k}'$,

$$\chi(\mathbf{q},t)=\sum_{\mathbf{k},\mathbf{k}'}\chi_{\mathbf{k}\mathbf{k}'}(\mathbf{q},t),$$
$$\chi_{\mathbf{k}\mathbf{k}'}(\mathbf{q},t)=\frac{i}{\hbar\Omega}\theta(t)\ll[\rho_{\mathbf{q}}^{\mathbf{k}}(t),\rho_{-\mathbf{q}}^{\mathbf{k}'}(0)]\gg, \tag{2}$$

where the double angular brackets represent a grand canonical ensemble average, Ω is the volume of the system, $\theta(t)$ is the step function, and we are using the Heisenberg picture. $\rho_{\mathbf{q}}^{\mathbf{k}}$ is the particle-hole operator, $\rho_{\mathbf{q}}^{\mathbf{k}}\equiv c_{\mathbf{k}-\mathbf{q}/2}^{\dagger}c_{\mathbf{k}+\mathbf{q}/2}$.

It is convenient to introduce a generalized relaxation function $R_{\mathbf{k}\mathbf{k}'}(\mathbf{q},t)$ which describes the relaxation of the system if a constant external perturbation coupling for times $t<0$ to the $\mathbf{k}'$ degree of freedom is suddenly switched off at $t=0$. $R_{\mathbf{k}\mathbf{k}'}(\mathbf{q},t)$ is the relaxation of the $\mathbf{k}'$ degree of freedom for $t>0$. The generalized response function [Eq. (2)] can be recovered from the relaxation function [see Eq. (B5) in Appendix B]. The advantage of using the relaxation function is that it satisfies a kinetic equation of motion [see Eq. (C9)].

The kinetic-equation approach has been extensively applied to both classical[17] and quantum many-body systems.[14,15] In the time domain the kinetic equation[12] is of the familiar Langevin form,

$$i\frac{d}{dt}R_{\mathbf{k}\mathbf{k}'}(\mathbf{q},t)=\frac{\hbar}{m}\mathbf{q}\cdot\mathbf{k}R_{\mathbf{k}\mathbf{k}'}(\mathbf{q},t)+\sum_{\mathbf{k}''}\int_0^t dt'\,M_{\mathbf{k}\mathbf{k}''}(\mathbf{q},t-t')\times R_{\mathbf{k}''\mathbf{k}'}(\mathbf{q},t'). \tag{3}$$

In Appendixes A–C we outline the derivation of the kinetic equation with the primary purpose of introducing a formal definition of the microscopic memory function which will serve as the starting point for our approximations. $M_{\mathbf{k}\mathbf{k}'}(\mathbf{q},t)$ carries information on how states of the system at earlier times affect the relaxation function $R_{\mathbf{k}\mathbf{k}'}(\mathbf{q},t)$ at the present time t.

In an exact formulation each matrix element of $M_{\mathbf{k}\mathbf{k}'}(\mathbf{q},t)$ is in general a different function of $\mathbf{q}$ and t, reflecting the property that each microscopic degree of freedom evolves slightly differently. However, in any practical calculation we need to group these matrix elements and approximate each group by a single function.

Before discussing approximations to the infinite array of matrix elements $M_{\mathbf{k}\mathbf{k}'}(\mathbf{q},t)$ we note that from the definition of $M_{\mathbf{k}\mathbf{k}'}(\mathbf{q},t)$ [see Eq. (C7)] it is straightforward to establish that the exact memory function matrix satisfies the condition

$$\sum_{\mathbf{k}}M_{\mathbf{k}\mathbf{k}'}(\mathbf{q},t)=0. \tag{4}$$

This is an important constraint on any approximation for $M_{\mathbf{k}\mathbf{k}'}(\mathbf{q},t)$ since the equation of continuity follows from it [see Eq. (C11) in Appendix C].

The physical constraints on $M_{\mathbf{k}\mathbf{k}'}(\mathbf{q},t)$ are quite different depending on the wave number $\mathbf{q}$. For small $\mathbf{q}$, the dominant contributions to $M_{\mathbf{k}\mathbf{k}'}(\mathbf{q},t)$ are given by the coupling between collective (hydrodynamic) degrees of freedom in the system, represented by the density $\rho_{\mathbf{q}}$ and the current density $J_{\mathbf{q}}$. On the other hand, as $\mathbf{q}$ increases the single-particle aspect of excitations becomes increasingly important and the electron $\mathbf{k}$ has to be treated as a distinct excitation (as opposed to being part of a collective motion) during its propagation through the medium. In the limit of very large $\mathbf{q}$ an electron will undergo frequent binary collisions with surrounding particles and its motion can be described by a Boltzmann-like equation. For intermediate values of $\mathbf{q}$ both the collective and single-particle aspects of the motion have to be treated together.

We can deal with this by representing $M_{\mathbf{k}\mathbf{k}'}(\mathbf{q},t)$ as a sum of two functions $M^s_{\mathbf{k}\mathbf{k}'}(\mathbf{q},t)$ and $M^c_{\mathbf{k}\mathbf{k}'}(\mathbf{q},t)$. For $M^s_{\mathbf{k}\mathbf{k}'}(\mathbf{q},t)$ we use approximations to $M_{\mathbf{k}\mathbf{k}'}(\mathbf{q},t)$ appropriate for our picture of the passage of a single particle through the randomly fluctuating surrounding medium. $M^c_{\mathbf{k}\mathbf{k}'}(\mathbf{q},t)$ contains the remaining part of the memory function. We will assume later that $M^c_{\mathbf{k}\mathbf{k}'}(\mathbf{q},t)$ describes the effective coupling between the density and current degrees of freedom of the system due to excitations of multiparticle modes.

With this separation of $M_{\mathbf{k}\mathbf{k}'}(\mathbf{q},t)$ into two parts, the kinetic equation, Eq. (C9), can also be split into two coupled equations, one involving only $M^s_{\mathbf{k}\mathbf{k}'}(\mathbf{q},z)$, and the other $M^c_{\mathbf{k}\mathbf{k}'}(\mathbf{q},z)$:

$$(z-\omega_{\mathbf{q}}^{\mathbf{k}})R^s_{\mathbf{k}\mathbf{k}'}(\mathbf{q},z)=i\delta_{\mathbf{k}\mathbf{k}'}+\sum_{\mathbf{k}_1}M^s_{\mathbf{k}\mathbf{k}_1}(\mathbf{q},z)R^s_{\mathbf{k}_1\mathbf{k}'}(\mathbf{q},z),$$
$$R_{\mathbf{k}\mathbf{k}'}(\mathbf{q},z)=R^s_{\mathbf{k}\mathbf{k}'}(\mathbf{q},z)-i\sum_{\mathbf{k}_1,\mathbf{k}_2}R^s_{\mathbf{k}\mathbf{k}_1}(\mathbf{q},z)M^c_{\mathbf{k}_1\mathbf{k}_2}(\mathbf{q},z)R_{\mathbf{k}_2\mathbf{k}'}(\mathbf{q},z), \tag{5}$$

where $\hbar\omega_{\mathbf{q}}^{\mathbf{k}}=\varepsilon^0_{\mathbf{k}+\mathbf{q}/2}-\varepsilon^0_{\mathbf{k}-\mathbf{q}/2}=\hbar^2\mathbf{k}\cdot\mathbf{q}/m$ is the difference in the free-single-particle energies $\varepsilon^0_{\mathbf{k}}$.

The single-particle relaxation function $R^s_{\mathbf{k}\mathbf{k}'}(\mathbf{q},z)$ is associated with the propagation of a single electron scattering off its surroundings. The relaxation function $R^s_{\mathbf{k}\mathbf{k}'}(\mathbf{q},z)$ and the single-particle response function $\chi^s_{\mathbf{k}\mathbf{k}'}(\mathbf{q})$ are related by an expression analogous to Eq. (B5) in Appendix B,

$$\chi^s_{\mathbf{k}\mathbf{k}'}(\mathbf{q},z)=\sum_{\mathbf{k}''}[\delta_{\mathbf{k}\mathbf{k}''}+izR^s_{\mathbf{k}\mathbf{k}''}(\mathbf{q},z)]\chi^s_{\mathbf{k}''\mathbf{k}'}(\mathbf{q}),$$
$$\chi^s(\mathbf{q},z)=\sum_{\mathbf{k},\mathbf{k}'}\chi^s_{\mathbf{k}\mathbf{k}'}(\mathbf{q},z). \tag{6}$$

We take $\chi^s_{\mathbf{k}\mathbf{k}'}(\mathbf{q})$ to be

$$\chi^s_{\mathbf{k}\mathbf{k}'}(\mathbf{q})=-\frac{1}{\hbar\Omega}\frac{n_{\mathbf{q}}^{\mathbf{k}}}{\omega_{\mathbf{q}}^{\mathbf{k}}}\delta_{\mathbf{k}\mathbf{k}'},$$
$$\chi^s(\mathbf{q})=\sum_{\mathbf{k},\mathbf{k}'}\chi^s_{\mathbf{k}\mathbf{k}'}(\mathbf{q}), \tag{7}$$

where $n_{\mathbf{q}}^{\mathbf{k}} = n(\mathbf{k}+\mathbf{q}/2) - n(\mathbf{k}-\mathbf{q}/2)$ is the difference in the single-particle occupation numbers in the ground state. If the occupation numbers $n(\mathbf{k})$ are taken to be step functions then $\chi^s(\mathbf{q})$ is the static response function of the noninteracting electron gas[3] $\chi^0(\mathbf{q})$.

It is clear that if we were to set $M^s_{\mathbf{k}\mathbf{k}'}(\mathbf{q},z)$ equal to zero then $\chi^s_{\mathbf{k}\mathbf{k}'}(\mathbf{q},z)$ obtained from the $R^s_{\mathbf{k}\mathbf{k}'}(\mathbf{q},z)$ would describe the free propagation of a single electron-hole pair.

For $M^s_{\mathbf{k}\mathbf{k}'}(\mathbf{q},z)$ we assume every random scattering process for a given $\mathbf{q}$ has the same relaxation time,

$$M^s_{\mathbf{k}\mathbf{k}'}(\mathbf{q},z) = \gamma^s(\mathbf{q},z)\left(\delta_{\mathbf{k}\mathbf{k}'} + \frac{n_{\mathbf{q}}^{\mathbf{k}}}{\hbar\Omega\chi^s(\mathbf{q})\omega_{\mathbf{q}}^{\mathbf{k}}}\right). \tag{8}$$

The last term in the expression is put there to ensure that $M^s_{\mathbf{k}\mathbf{k}'}(\mathbf{q},z)$ satisfies conservation requirements [see Eq. (4)]. The form of the function $\gamma^s(\mathbf{q},z)$, which is independent of $\mathbf{k}$ and $\mathbf{k}'$, is specified later on. For now we note that for a particle making its way through a field of scatterers (such as phonons or impurities), $\gamma^s(\mathbf{q},z)$ would describe the relaxation of the current, leading to a finite diffusion constant in the hydrodynamic limit. In the case of classical liquids, $\gamma^s(\mathbf{q},z)$ incorporates the so-called cage effect where a single particle tends to be trapped by the particles surrounding it. This type of approximation for the memory function was first introduced by Götze.[16] If we were to approximate $\gamma^s(\mathbf{q},z)$ by a single relaxation time τ_s^{-1} for all $\mathbf{q}$ and z, then the resulting $R^s_{\mathbf{k}\mathbf{k}'}(\mathbf{q},z)$ would correspond to the solution of the relaxation-time approximation for the Boltzmann equation. This is consistent with our physical picture of $R^s_{\mathbf{k}\mathbf{k}'}(\mathbf{q},z)$ as the relaxation function describing a single particle propagating through randomly fluctuating surroundings.

We now introduce the assumption that the collective memory function $M^c_{\mathbf{k}\mathbf{k}'}(\mathbf{q},z)$ couples only the density and current degrees of freedom. With this assumption it can be shown (see Appendix D) that

$$M^c_{\mathbf{k}\mathbf{k}'}(\mathbf{q},z) = \frac{n_{\mathbf{q}}^{\mathbf{k}}}{\hbar\beta|\mathbf{q}|}\left(M^c_{J_\rho}(\mathbf{q}) - M^c_{JJ}(\mathbf{q},z)\frac{\omega_{\mathbf{q}}^{\mathbf{k}'}}{|\mathbf{q}|}\right). \tag{9}$$

Equations (8) and (9) reduce the task of evaluating an infinite array of different matrix elements $M_{\mathbf{k}\mathbf{k}'}(\mathbf{q},t)$ to the more tractable level of needing to determine just three functions $M^c_{J_\rho}(\mathbf{q})$, $M^c_{JJ}(\mathbf{q},z)$, and $\gamma^s(\mathbf{q},z)$.

$M^c_{J_\rho}(\mathbf{q})$ is shown in Appendix E to be closely related to the static effective interaction $v_{\mathbf{q}}^{\text{eff}}$,

$$M^c_{J_\rho}(\mathbf{q}) = -\frac{\beta|\mathbf{q}|}{\Omega}v_{\mathbf{q}}^{\text{eff}}. \tag{10}$$

The static effective interaction $v_{\mathbf{q}}^{\text{eff}}$ incorporates the static density depletion effects of the instantaneous exchange-correlation hole around an electron. Being static it can depend only on ground-state properties of the system which are known from numerical simulation data.[18]

$M^c_{JJ}(\mathbf{q},z)$ can be written in the form (see Appendix F),

$$M^c_{JJ}(\mathbf{q},z) = \frac{\beta m}{\Omega n}[\gamma(\mathbf{q},z) - \gamma^s(\mathbf{q},z)], \tag{11}$$

where n is the mean density of the system. $\gamma(\mathbf{q},z)$ describes the coupling of the current fluctuations (both hydrodynamic and single-particle) to the multiparticle excitations. Subtracting off $\gamma^s(\mathbf{q},z)$ ensures that $M^c_{\mathbf{k}\mathbf{k}'}(\mathbf{q},z)$ contains no part of the single-particle component which is included already in $M^s_{\mathbf{k}\mathbf{k}'}(\mathbf{q},z)$.

We use the mode-mode coupling approximation to determine $\gamma(\mathbf{q},z)$. We assume that at $t=0$ the density fluctuation interacts with its surroundings inducing a second density fluctuation within the surroundings. The two fluctuations are then assumed to propagate independently, until at later time t they mutually interact for a second time. In this way a disturbance induced in the surroundings can later return to influence the motion of the original density fluctuation.

We introduce the function $\bar{\gamma}(\mathbf{q},t)$,

$$\gamma(\mathbf{q},z) = \int_{-\infty}^{\infty}\frac{d\omega}{2\pi}\frac{1}{\omega(z-\omega)}\int_{-\infty}^{\infty}dt\, e^{-i\omega t}\bar{\gamma}(\mathbf{q},t). \tag{12}$$

In Appendix F, Eq. (F6) gives an exact expression for $\bar{\gamma}(\mathbf{q},t)$, relating it to a higher correlation function. We show there that it can be approximated within the framework of mode-mode coupling by

$$\bar{\gamma}(\mathbf{q},t) = \frac{1}{\Omega}\int d\mathbf{r}_1 d\mathbf{r}_1' d\mathbf{r}_2 d\mathbf{r}_2' e^{i\mathbf{q}\cdot(\mathbf{r}_1'-\mathbf{r}_1)}[\mathbf{q}\cdot\nabla v(\mathbf{r}_1'-\mathbf{r}_2')]g(\mathbf{r}_1'-\mathbf{r}_2')$$
$$\times[S(\mathbf{r}_1',t;\mathbf{r}_1,0)S(\mathbf{r}_2',t;\mathbf{r}_2,0) + S(\mathbf{r}_2',t;\mathbf{r}_1,0)S(\mathbf{r}_1',t;\mathbf{r}_2,0)][\mathbf{q}\cdot\nabla v(\mathbf{r}_2-\mathbf{r}_1)]g(\mathbf{r}_2-\mathbf{r}_1). \tag{13}$$

The van Hove density-density correlation function $S(\mathbf{r},t;\mathbf{r}',t')$ is the Fourier transform of the dynamic structure factor $S(\mathbf{q},\omega)$ and $g(\mathbf{r})$ is the instantaneous pair-correlation function.

Equation (13) describes a density fluctuation at $\mathbf{r}_2$ coupling to the surroundings at time $t=0$. The coupling induces a density fluctuation in the surroundings at $\mathbf{r}_1$. The pair-correlation function $g(\mathbf{r}_1-\mathbf{r}_2)$ takes into account the correlation between the two density fluctuations incorporating the shape of the exchange-correlation hole. The terms $[S(\mathbf{r}_1',t;\mathbf{r}_1,0)S(\mathbf{r}_2',t;\mathbf{r}_2,0)]$ describe the independent propagation of the two density fluctuations from positions $\mathbf{r}_1$ and $\mathbf{r}_2$ at time $t=0$ to $\mathbf{r}_1'$ and $\mathbf{r}_2'$ at time t. At t the two fluctuations interact for a second time, and again they are correlated by an instantaneous correlation function $g(\mathbf{r}_1'-\mathbf{r}_2')$. Note that the $g(\mathbf{r})$ functions

correlate different fluctuations at the same instant of time while the $S(\mathbf{r}',t';\mathbf{r},t)$ functions correlate the same density fluctuation at two different times.

We turn now to the single-particle memory function $\gamma^s(\mathbf{q},z)$. This is determined by a single-particle excitation dynamically coupling to its surrounding exchange-correlation hole. The excitations induced in the surroundings can contain both collective and single-particle effects. Introducing the function $\bar{\gamma}^s(\mathbf{q},t)$ for the time domain analogously to Eq. (12) shows that we can write

$$\begin{aligned}\bar{\gamma}^s(\mathbf{q},t) = \frac{1}{\Omega}\int d\mathbf{r}_1 d\mathbf{r}_1' d\mathbf{r}_2 d\mathbf{r}_2' e^{i\mathbf{q}\cdot(\mathbf{r}_1'-\mathbf{r}_1)} \\ \times[\mathbf{q}\cdot\nabla v(\mathbf{r}_1'-\mathbf{r}_2')]g(\mathbf{r}_1'-\mathbf{r}_2') \\ \times S^s(\mathbf{r}_1',t;\mathbf{r}_1,0)S(\mathbf{r}_2',t;\mathbf{r}_2,0) \\ \times[\mathbf{q}\cdot\nabla v(\mathbf{r}_2-\mathbf{r}_1)]g(\mathbf{r}_2-\mathbf{r}_1). \quad (14)\end{aligned}$$

The single-particle density-density correlation function $S^s(\mathbf{r},t;\mathbf{0},0)$ represents the time evolution of a density fluctuation $\delta\rho(\mathbf{r},t)$ from which the collective component has been projected out. $S^s(\mathbf{r},t;\mathbf{0},0)$ is specified by the single-particle part of the relaxation function $R^s_{\mathbf{k}\mathbf{k}'}(\mathbf{q},z)$ through the fluctuation-dissipation theorem.

In Eq. (14) the effect of the single-particle motion on the motion of its surroundings and vice versa has been introduced by coupling the two correlation functions, $S(\mathbf{r},t;\mathbf{0},0)$ and $S^s(\mathbf{r},t;\mathbf{0},0)$ at times $t=0$ and t. Equation (14), like Eq. (13), describes the interaction and independent propagation of two density fluctuations, but here the two fluctuations are distinguishable.

Using our expressions for $M^s_{\mathbf{k}\mathbf{k}'}(\mathbf{q},z)$ and $M^c_{\mathbf{k}\mathbf{k}'}(\mathbf{q},z)$ [Eqs. (8) and (9)], we obtain simple equations for the total response function $\chi(\mathbf{q},z)$ and the single-particle response function $\chi^s(\mathbf{q},z)$. Their solution is

$$\begin{aligned}\chi^s(\mathbf{q},z) &= \frac{\chi^\gamma(\mathbf{q},z)}{1-i\gamma^s(\mathbf{q},z)R^\gamma(\mathbf{q},z)}\,, \\ \chi(\mathbf{q},z) &= \frac{\chi^s(\mathbf{q},z)}{1+\left(v_{\mathbf{q}}^{\rm eff}+\frac{mz}{nq^2}[\gamma(\mathbf{q},z)-\gamma^s(\mathbf{q},z)]\right)\chi^s(\mathbf{q},z)}\,,\end{aligned} \quad (15)$$

where

$$\begin{aligned}\chi^\gamma(\mathbf{q},z) &= \frac{1}{\hbar\Omega}\sum_{\mathbf{k}}\frac{n_{\mathbf{q}}^{\mathbf{k}}}{z-\omega_{\mathbf{q}}^{\mathbf{k}}-\gamma^s(\mathbf{q},z)}\,, \\ R^\gamma(\mathbf{q},z) &= \frac{-i}{\hbar\Omega\chi^s(\mathbf{q})}\sum_{\mathbf{k}}\frac{n_{\mathbf{q}}^{\mathbf{k}}}{\omega_{\mathbf{q}}^{\mathbf{k}}}\frac{1}{z-\omega_{\mathbf{q}}^{\mathbf{k}}-\gamma^s(\mathbf{q},z)}.\end{aligned} \quad (16)$$

If we set $\gamma^s(\mathbf{q},z)=0$ then $\chi^s(\mathbf{q},z)$ would become the Lindhard function $\chi^0(\mathbf{q},z)$. The term $v_{\mathbf{q}}^{\rm eff}+(mz/nq^2)\gamma(\mathbf{q},z)$ in the denominator of $\chi(\mathbf{q},z)$ would then give us a microscopically derived dynamic local-field correction.

Using the fluctuation-dissipation theorem our expressions for $\gamma^s(\mathbf{q},z)$ and $\gamma(\mathbf{q},z)$ [Eqs. (13) and (14)] can be written in terms of $\chi^s(\mathbf{q},z)$ and $\chi(\mathbf{q},z)$,

$$\begin{aligned}\gamma(\mathbf{q},z) = \frac{4\hbar}{nm}\int_{-\infty}^{\infty}\frac{d\omega}{2\pi(z-\omega)\omega}\int_0^\omega\frac{d\omega'}{2\pi}\sum_{\mathbf{q}'}(\hat{\mathbf{q}}\cdot\mathbf{q}')\bar{v}_{\mathbf{q}'}[{\rm Im}\chi(\mathbf{q}',\omega'){\rm Im}\chi(\mathbf{q}-\mathbf{q}',\omega-\omega')] \\ \times[(\hat{\mathbf{q}}\cdot\mathbf{q}')\bar{v}_{\mathbf{q}'}+\bar{v}_{\mathbf{q}-\mathbf{q}'}(|\mathbf{q}|-\hat{\mathbf{q}}\cdot\mathbf{q}')], \\ \gamma^s(\mathbf{q},z) = \frac{4\hbar}{nm}\int_{-\infty}^{\infty}\frac{d\omega}{2\pi(z-\omega)\omega}\int_0^\omega\frac{d\omega'}{2\pi}\sum_{\mathbf{q}'}(\hat{\mathbf{q}}\cdot\mathbf{q}')\bar{v}_{\mathbf{q}'}[{\rm Im}\chi(\mathbf{q}',\omega'){\rm Im}\chi^s(\mathbf{q}-\mathbf{q}',\omega-\omega')][(\hat{\mathbf{q}}\cdot\mathbf{q}')\bar{v}_{\mathbf{q}'}].\end{aligned} \quad (17)$$

$\bar{v}_{\mathbf{q}}$ is the Fourier transform of $\bar{v}(\mathbf{r})$ which is defined as [see Eq. (13)],

$$\nabla\bar{v}(\mathbf{r}) \equiv g(\mathbf{r})\nabla v(\mathbf{r}). \quad (18)$$

It is straightforward to show[4] that

$$\begin{aligned}\bar{v}_{\mathbf{q}} &= v_{\mathbf{q}}\,[1-\bar{G}(\mathbf{q})], \\ \bar{G}(\mathbf{q}) &= -\frac{1}{n}\int\frac{d^3q'}{(2\pi)^3}\hat{\mathbf{q}}\cdot\hat{\mathbf{q}}'[S(|\mathbf{q}-\mathbf{q}'|)-1].\end{aligned} \quad (19)$$

Equations (15) and (17) form a closed set. We solve these iteratively until the solutions become self-consistent.

III. RESULTS

Tanatar and Ceperley[18] have carried out numerical simulations of the ground-state properties of the two-dimensional electron system for densities down to $r_s \sim 40$. Their published results include the pair-correlation function $g(\mathbf{r})$, which is the probability of finding two electrons separated by distance $\mathbf{r}$ at the same instant of time. By Fourier transforming these data we have extracted the static structure factor $S(\mathbf{q})$ (see Fig. 1). Determining $S(\mathbf{q})$ in this way is not accurate for small $|\mathbf{q}|$, and in this region we have constructed $S(\mathbf{q})$ so that it gives the value of the compressibility obtained from their ground-state energy.

The fluctuation-dissipation theorem relates $S(\mathbf{q})$ to the

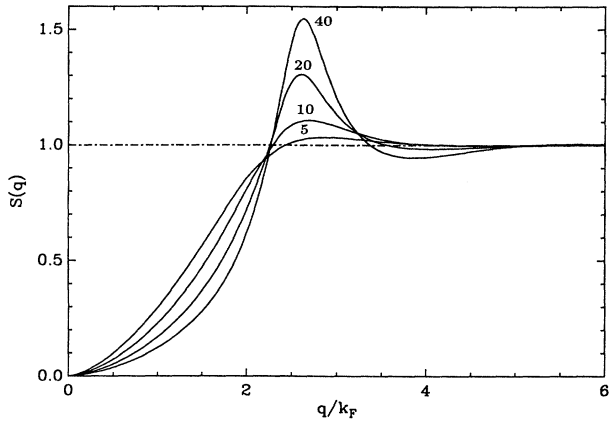

FIG. 1. The static structure factor $S(\mathbf{q})$ for electron densities $r_s = 5$, 10, 20, and 40, deduced from pair correlation functions data in Ref. 18.

imaginary part of $\chi(\mathbf{q},\omega)$,

$$S(\mathbf{q}) = \frac{\hbar}{\pi n}\int_0^\infty d\omega\, \mathrm{Im}\chi(\mathbf{q},\omega). \tag{20}$$

Once we independently know $S(\mathbf{q})$, we can use the expressions Eqs. (20) and (15) to uniquely determine the static effective interaction $v_{\mathbf{q}}^{\mathrm{eff}}$. Since with every iteration the functions $\gamma(\mathbf{q},z)$ and $\gamma^s(\mathbf{q},z)$ change, $v_{\mathbf{q}}^{\mathrm{eff}}$ must be readjusted each time in order to leave $S(\mathbf{q})$ unchanged.

It is a common practice to express $v_{\mathbf{q}}^{\mathrm{eff}}$ in terms of a Hubbard-type local field $G(\mathbf{q})$, where $v_{\mathbf{q}}^{\mathrm{eff}} = v_{\mathbf{q}}[1 - G(\mathbf{q})]$. Figure 2 shows $G(\mathbf{q})$ for electron densities from $r_s = 5$ to 40. Also shown is $G^0(\mathbf{q})$ for the initial iteration for which $\gamma(\mathbf{q},z)$ and $\gamma^s(\mathbf{q},z)$ are zero. Even for $r_s = 5$ the maximum value of $G(\mathbf{q})$ exceeds unity, corresponding to an attractive region for $v_{\mathbf{q}}^{\mathrm{eff}}$ around $|\mathbf{q}|/k_F \sim 2.6$. This is a result of correlations excluding charge from the immediate neighborhood of the electron. Since the overall number of particles is conserved the excluded charge must go somewhere, and it is pushed to the outside of the exchange-correlation hole, resulting in a pile-up of charge there. When the density in this shell exceeds the mean density of the system, v^{eff} can have an attractive part.

Tanatar and Ceperley also give some results for $r_s \lesssim 10$ for the occupation numbers $n(\mathbf{k} \pm \mathbf{q}/2)$ which determine our function $n_{\mathbf{q}}^{\mathbf{k}}$. We have found that our results are not greatly altered if these functions are replaced by step functions. Because of this, and because no data is available for $r_s > 10$, for our final results we have approximated the $n(\mathbf{k} \pm \mathbf{q}/2)$ by step functions.

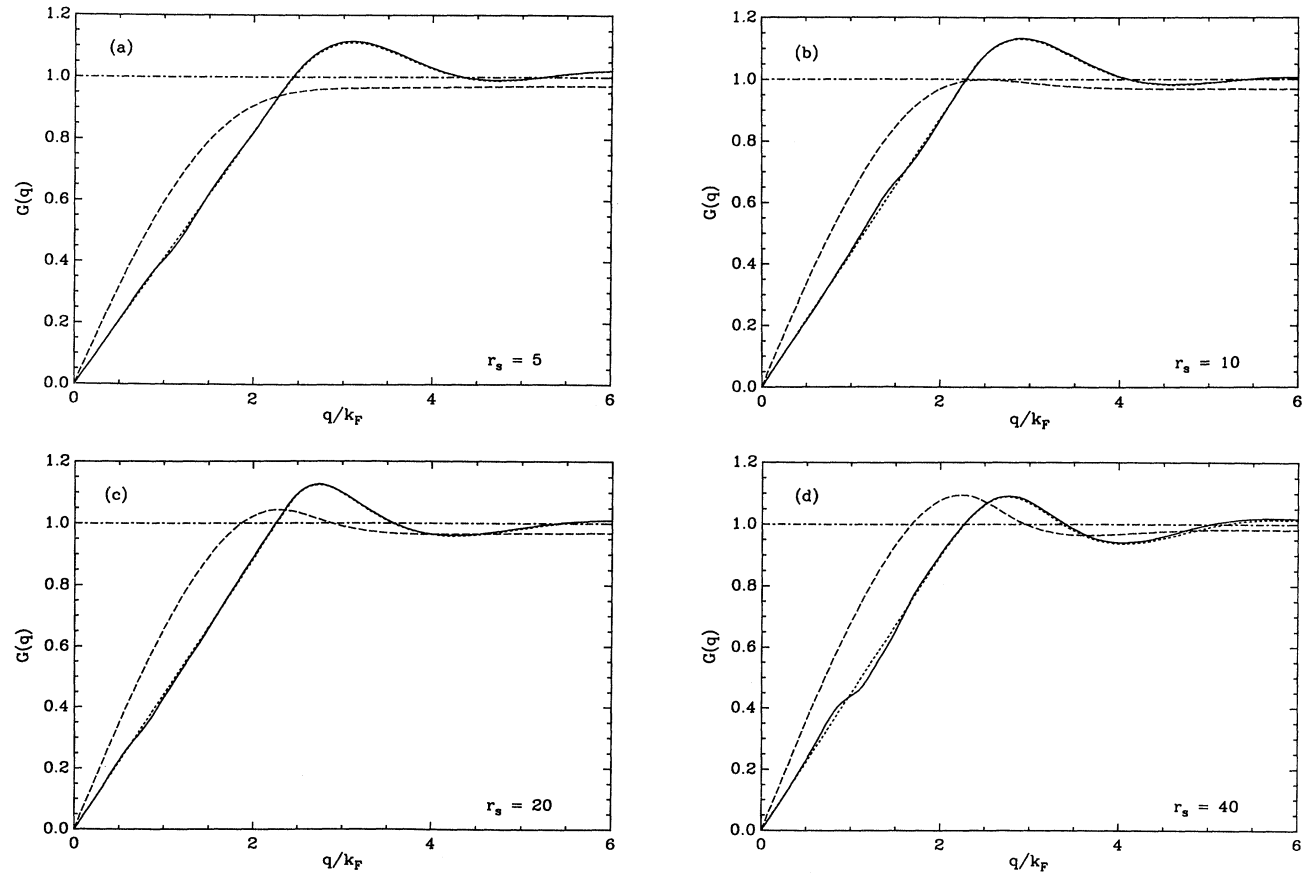

FIG. 2. Static local field $G(\mathbf{q})$ for densities $r_s = 5$, 10, 20, and 40 (solid line). The dotted line is $G^0(\mathbf{q})$ when memory function effects are ignored. The dashed line is $\bar{G}(\mathbf{q})$ calculated from Eq. (19).

Figure 3 shows the functions $\gamma(\mathbf{q},z)$ and $\gamma^s(\mathbf{q},z)$ [see Eq. (11)] for densities $r_s = 5$ and 40. Recalling Eq. (15) for $\chi(\mathbf{q},\omega)$, we see that for $r_s = 5$ the values of $\gamma(\mathbf{q},\omega)$ and $\gamma^s(\mathbf{q},\omega)$ are so small that they have little effect on the overall shape of the response function. However for r_s =40 the peaks in $\gamma(\mathbf{q},\omega)$ and $\gamma^s(\mathbf{q},\omega)$ are of the order of $\hbar\omega_F$, and in this case $\chi(\mathbf{q},\omega)$ is significantly affected.

In Fig. 4 the imaginary part of the response functions $\chi(\mathbf{q},\omega)$ are shown. For $r_s = 5$ the narrow plasmon peak in the small $q-\omega$ region saturates the available spectral strength, making the single-particle contributions in this region practically invisible on this scale. The peak has a narrow but finite width.

[We recall that within the RPA that the plasmon is a long-wavelength excitation of zero width. For the two-dimensional system its frequency $\omega_p(\mathbf{q})$ vanishes as $|\mathbf{q}|^{1/2}$ for $|\mathbf{q}|$ going to zero. As $|\mathbf{q}|$ increases the RPA plasmon dispersion curve only asymptotically approaches the boundary of the single-particle excitation region,[19] and so the plasmon cutoff momentum q_c^{RPA} is much larger than k_F for the lower densities. In the RPA there are no multiparticle excitations and so the plasmon width $\Delta\omega(\mathbf{q})$ is identically zero for all $|\mathbf{q}| < q_c^{\mathrm{RPA}}$.]

The finite width of our plasmon resonance arises from contributions to the spectral strength which are multiparticle in origin. Multiparticle excitations are also responsible for the tails which are appended to the central envelope of $\mathrm{Im}\chi(\mathbf{q},\omega)$. Because the dispersion curve is much flatter than in RPA, the plasmon cutoff momentum $q_c/k_F \sim 1$ is much smaller than RPA. This effect is primarily due to the static correlations represented by $v_{\mathbf{q}}^{\mathrm{eff}}$.

At $r_s = 20$ the multiparticle tails at small and large ω are more pronounced. The plasmon peak is broader. If we increase $\mathbf{q}$, the plasmon merges with the single-particle spectrum at $q_c \sim 1.7$. Then at around $|\mathbf{q}|/k_F \simeq 2.6$ another peak appears on the opposite low-ω side of the single-particle spectrum.

By $r_s = 40$ all these effects have become much more pronounced, and in particular the additional peak around $|\mathbf{q}|/k_F \simeq 2.6$ is quite sharp. Figure 5 shows $\mathrm{Im}[v_{\mathbf{q}}\chi(\mathbf{q},\omega)]$ for $r_s = 40$ for momentum transfers $|\mathbf{q}|/k_F$ from 1.6 to 3.1 . It also shows $\mathrm{Im}[v_{\mathbf{q}}\chi(\mathbf{q},\omega)]$ without dynamic memory effects [that is with $\gamma(\mathbf{q},z)$ and $\gamma^s(\mathbf{q},z)$ set equal to zero, but retaining the static local field $G(\mathbf{q})$]. For $|\mathbf{q}|/k_F$=1.6 the plasmon peak has a fractional half-width of about 10%. Even though our plasmon cutoff for $r_s = 40$ is around $q = 1.8k_F$, the plasmon peak remains a well-defined excitation and continues to saturate the spectral strength. For $|\mathbf{q}|/k_F = 2.1$ the plasmon has

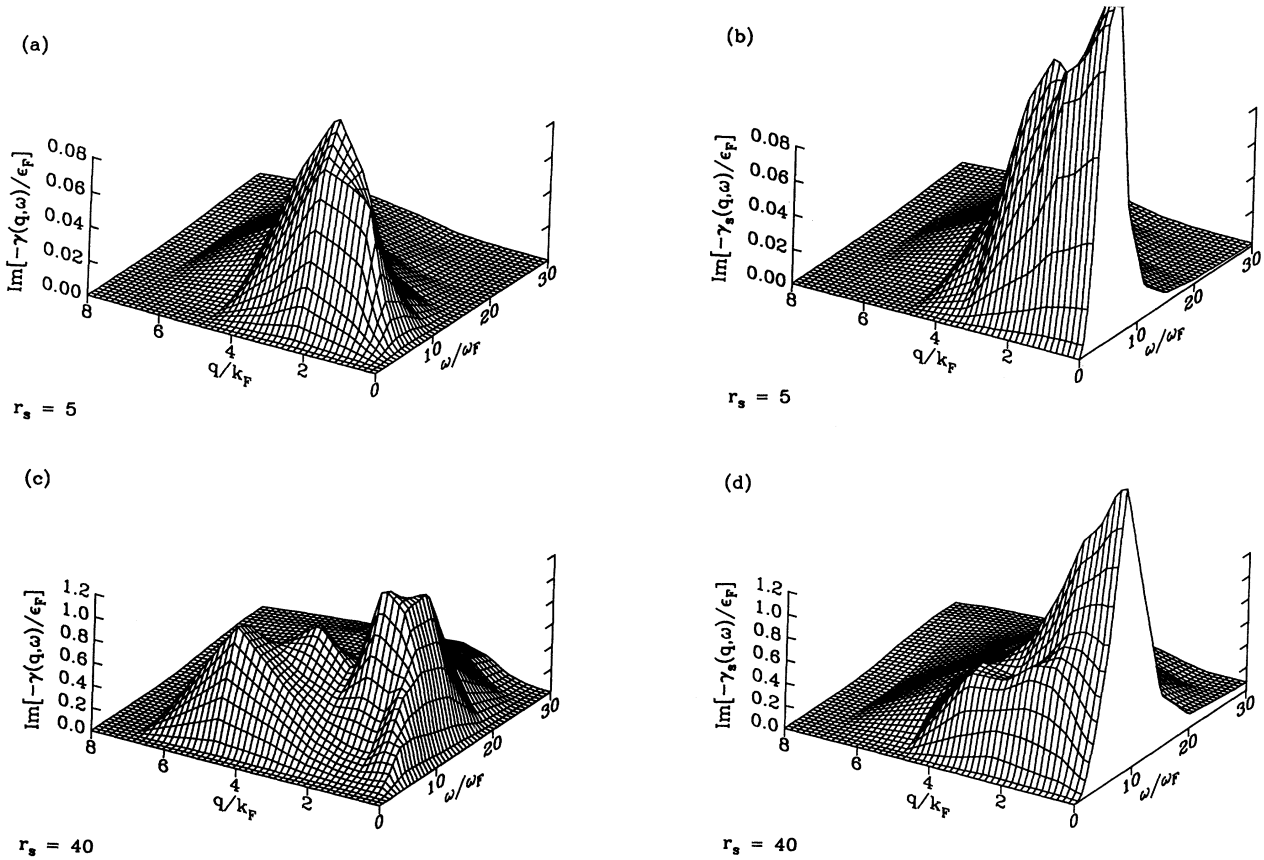

FIG. 3. (a) $\mathrm{Im}[-\gamma(\mathbf{q},\omega)]$ for $r_s = 5$. (b) $\mathrm{Im}[-\gamma^s(\mathbf{q},\omega)]$ for $r_s = 5$. (c) $\mathrm{Im}[-\gamma(\mathbf{q},\omega)]$ for $r_s = 40$. (d) $\mathrm{Im}[-\gamma^s(\mathbf{q},\omega)]$ for $r_s = 40$. For all $r_s \gtrsim 20$ the heights of the peaks are comparable to E_F, and these functions can significantly affect $\chi(\mathbf{q},\omega)$.

merged with the single-particle spectrum but the spectrum is still skewed towards high ω. At $|\mathbf{q}|/k_F = 2.28$ the spectral strength is almost completely symmetric in ω, apart from a distinct high-ω tail. For this value of $|\mathbf{q}|/k_F$ the function $[1 - G(\mathbf{q})]$ passes through zero (see Fig. 2), and so the dashed line coincides exactly with $\chi^0(\mathbf{q},\omega)$. For $|\mathbf{q}|/k_F = 2.6$ we see the new peak which develops on the low-ω side of $\chi(\mathbf{q},\omega)$. For $|\mathbf{q}|/k_F = 3.1$ the peak has disappeared but the spectral strength is still skewed towards low ω. The spectral strength goes over essentially to the noninteracting result by $|\mathbf{q}|/k_F \gtrsim 3.6$.

The origin of the second peak on the low-energy side of $\mathrm{Im}\chi(\mathbf{q},\omega)$ can be understood from the structure of our expression for the response function [Eq. (15)]. We have noted that for $r_s \gtrsim 5$ the local field $G(\mathbf{q})$ can exceed unity for some values of $\mathbf{q}$. In this case it is the region around $|\mathbf{q}|/k_F \simeq 2.6$ where the effective potential $v_{\mathbf{q}}^{\mathrm{eff}} = v_{\mathbf{q}}[1 - G(\mathbf{q})]$ is the most strongly attractive. The cause of this can be traced to the piling up of electrons at the edges of the exchange-correlation hole and the development of long-range correlations which are reflected in oscillations of the pair-correlation function $g(\mathbf{r})$ with a period matching the interparticle spacing. As r_s increases the peak in $G(\mathbf{q})$ grows sufficiently high that it is possible for the denominator of $\chi(\mathbf{q},\omega)$ to become very small or to change sign for positive $\chi^s(\mathbf{q},\omega)$. The likelihood of this happening increases markedly with decreasing density, not only because the peak in $G(\mathbf{q})$ is higher, but also because when Eq. (15) is expressed in dimensionless variables there is a prefactor of r_s in front of the $\chi^s(\mathbf{q},\omega)$ term in the denominator.

The presence of the low-energy peak in Fig. 4 indicates that for $r_s \gtrsim 20$ the system strongly favors excitations with a $\mathbf{q}$ value matching the reciprocal lattice vector of the Wigner crystal. The associated excitations are precursors of the phase transition to a Wigner crystal. As we approach the transition point we would expect a softening of the peak position towards $\omega = 0$. At the transition point the peak should diverge leading to a divergence in the static susceptibility $\chi(\mathbf{q})$ for $\mathbf{q}$ equal to the reciprocal lattice vector. In Fig. 6 we see that $\chi(\mathbf{q})$ does develop a very large peak.

We also observe a strong renormalization due to dynamical effects of the particle-hole propagator $\chi^\gamma(\mathbf{q},\omega)$ [see Eq. (16)]. $\chi^\gamma(\mathbf{q},\omega)$ describes propagation of the dressed particle and hole. For $\omega \to 0$ we have

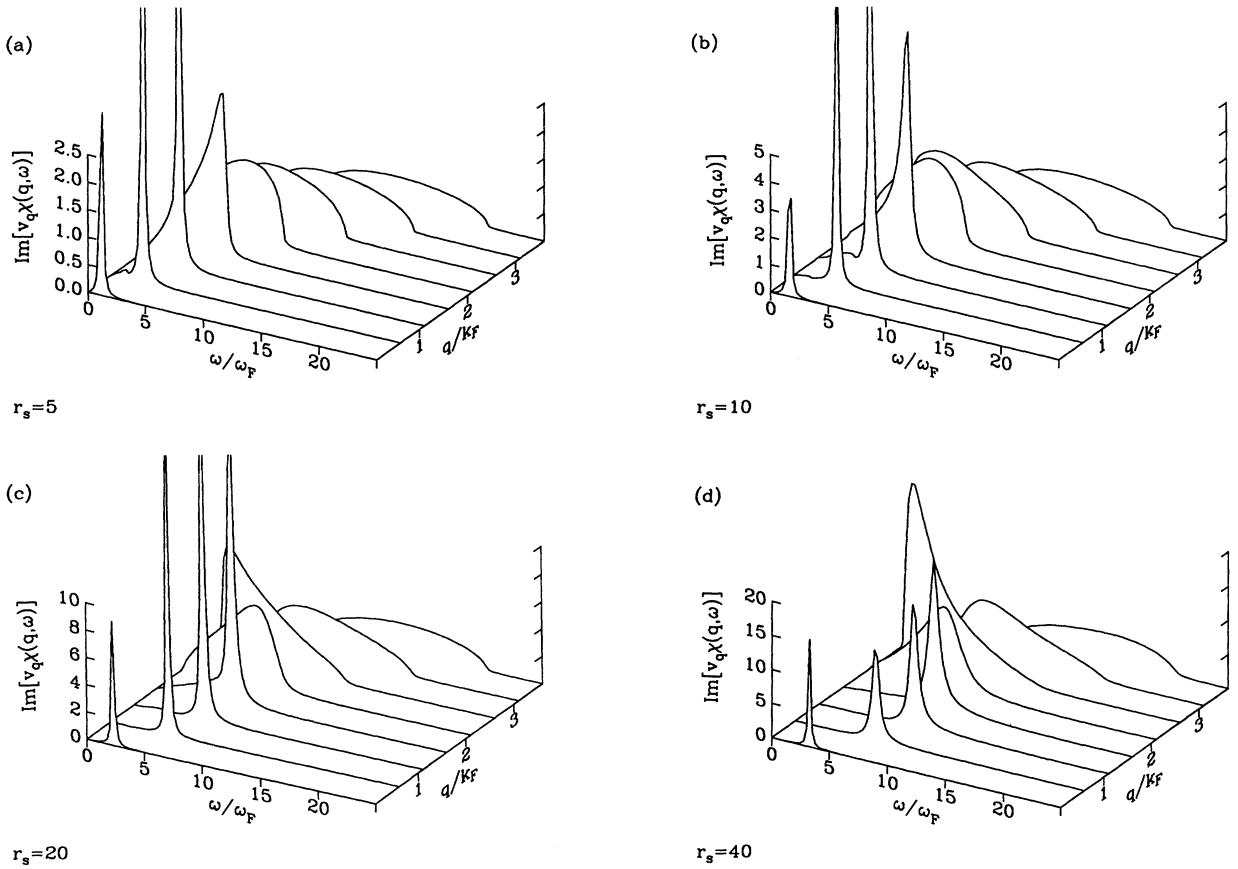

FIG. 4. $\mathrm{Im}[v_{\mathbf{q}}\chi(\mathbf{q},\omega)]$ for densities $r_s = 5$, 10, 20, and 40. For the lower densities the plasmon peak develops a significant width for all nonzero $\mathbf{q}$, and there are large- and small-ω tails on the single-particle contribution to $\chi(\mathbf{q},\omega)$. For $r_s = 20$ and 40 there is an additional peak on the low-ω side of the single-particle spectrum around $q/k_F \simeq 2.6$ and $\omega/\omega_F \simeq 1.8$.

$\mathrm{Im}\gamma^s(\mathbf{q},\omega) \sim \omega^2$ and $\mathrm{Re}\gamma^s(\mathbf{q},\omega) \sim \omega$, so for $\hbar\omega \ll \epsilon_F$

$$\chi^\gamma(\mathbf{q},\omega) = \frac{1}{\hbar\Omega a(\mathbf{q})} \sum_{\mathbf{k}} \frac{n_{\mathbf{q}}^{\mathbf{k}}}{\omega - \omega_{\mathbf{q}}^{\mathbf{k}}/a(\mathbf{q})} , \tag{21}$$

where $a(\mathbf{q}) = 1 - [d\,\mathrm{Re}\gamma^s(\mathbf{q},\omega)/d\omega]\,|_{\omega=0} > 1$. We would expect the renormalization to increase rapidly as the low-energy excitation peak softens towards $\omega = 0$. Figure 7 shows there is a marked jump in the renormalization when the density is changed from $r_s \sim 20$ to 40. For small $|\,\mathbf{q}\,| \ll k_F$ the function $a(\mathbf{q})$ can be interpreted as the electron effective mass m^*/m, although it is important to note that since we use the local-field approximation for the static properties, only dynamical renormalization

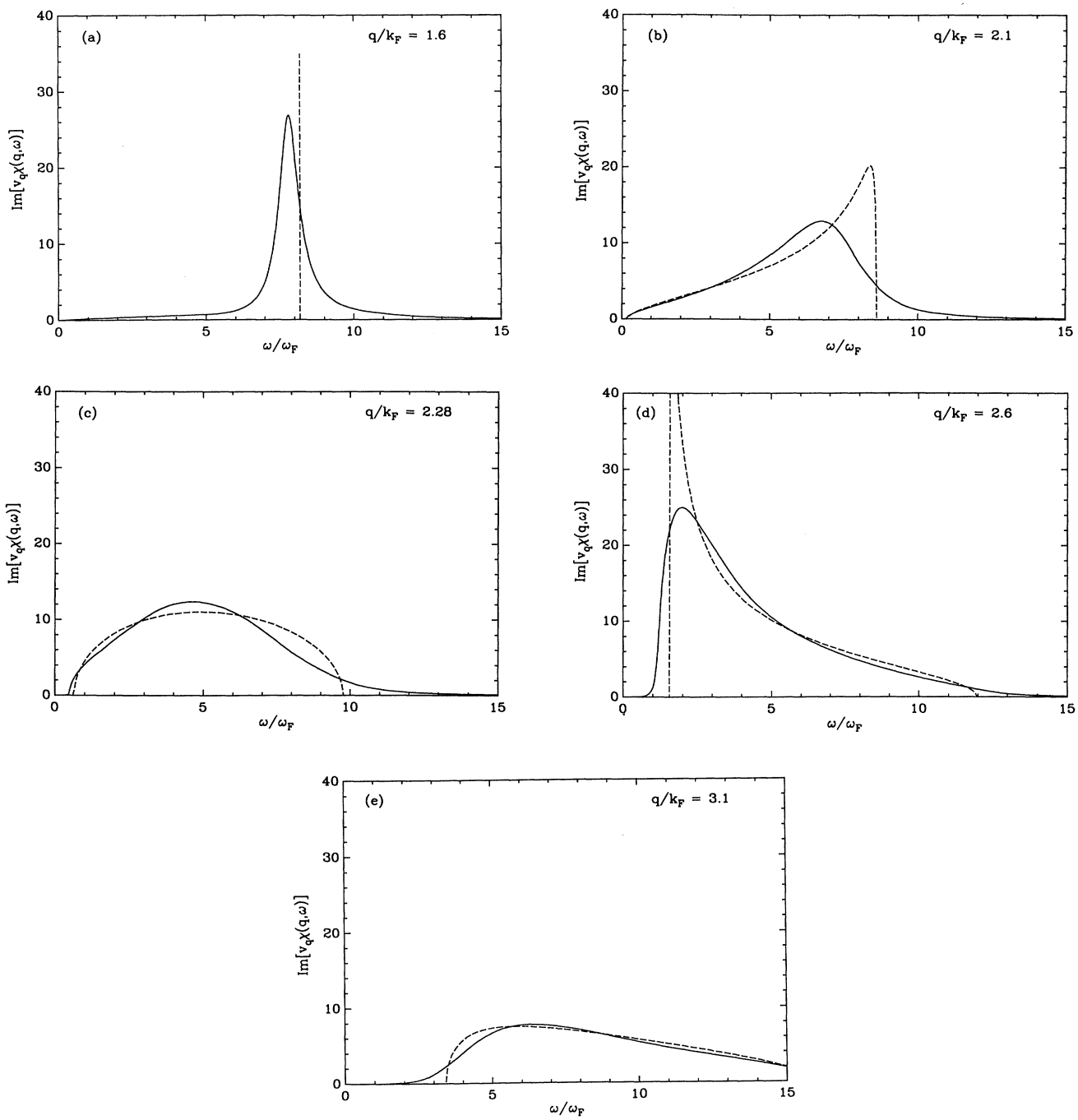

FIG. 5. $\mathrm{Im}[v_{\mathbf{q}}\chi(\mathbf{q},\omega)]$ for $r_s = 40$ for momentum transfers $|\mathbf{q}|/k_F = 1.6$, 2.1, 2.28, 2.6, and 3.1 (solid line). The dashed line is $\mathrm{Im}[v_{\mathbf{q}}\chi(\mathbf{q},\omega)]$ without dynamic memory effects [that is with $\gamma(\mathbf{q},z)$ and $\gamma^s(\mathbf{q},z)$ set equal to zero, but retaining the static local field $G(\mathbf{q})$]. At $|\mathbf{q}|/k_F = 2.28$, the function $[1 - G(\mathbf{q})]$ passes through zero (see Fig. 2), and so the dashed line is exactly $\chi^0(\mathbf{q},\omega)$.

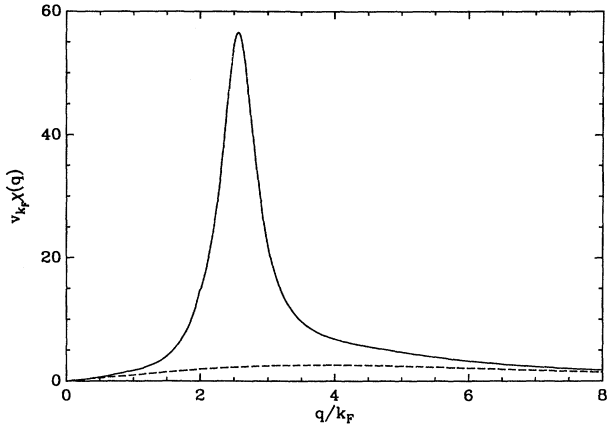

FIG. 6. $v_q\chi(\mathbf{q})$ for $r_s = 40$ (solid line) compared with $v_q\chi^{\mathrm{RPA}}(\mathbf{q})$ (dashed line). At the solidification density $\chi(\mathbf{q})$ peaks for $\mathbf{q}$ equal to the reciprocal lattice vector of the Wigner crystal.

effects are contained in $a(\mathbf{q})$.

Figure 8(a) shows the plasmon dispersion curves for densities from $r_s = 5$ to 40. Also shown are the curves when only the static correlations $v_{\mathbf{q}}^{\mathrm{eff}}$ are taken into account with the multiparticle effects $\gamma(\mathbf{q},\omega)$ and $\gamma^s(\mathbf{q},\omega)$ omitted. The RPA curves are given for reference.

For $r_s \gtrsim 10$ the plasmon curves are significantly below the RPA curves, and, unlike the RPA plasmon curves,[19] they intersect the single-particle excitation boundary at a sharp angle. This effect can be traced back to the ω tails which form on $\mathrm{Im}\chi^s(\mathbf{q},z)$ due to the $\gamma^s(\mathbf{q},z)$. The plasmon cutoff momenta q_c are much smaller than in the RPA.

The depression of the plasmon dispersion curves down to smaller ω is a consequence of the correlations between the electrons. These cut down the effective strength of the electron-electron interactions which has the effect of reducing the plasmon frequency. At higher densities the flattening of the curves is primarily due to the static correlations contained in $v_{\mathbf{q}}^{\mathrm{eff}}$. However for $r_s \gtrsim 20$ we find that the dynamic correlations represented by $\gamma(\mathbf{q},\omega)$ and especially $\gamma^s(\mathbf{q},\omega)$ do affect the dispersion curves leading to negative dispersion for large $\mathbf{q}$.

In Fig. 8(b) the fractional width at half-maximum $\Delta\omega(\mathbf{q})/\omega_p(\mathbf{q})$ of the plasmon resonance is shown. The finite width in our plasmon peak comes from the plasmon coupling to multiparticle excitations, an effect which is neglected within RPA. Holas and Singwi[20] have calculated the properties of the plasmon in the two-dimensional system for high densities, $r_s \lesssim 4$. They found that the plasmon width for this case remains less than or of the order of 1%, and we confirm that for $r_s \lesssim 10$ the fractional width remains less than a few percent up to the cutoff momentum q_c, so that the coupling to the multiparticle excitations remains weak. How-

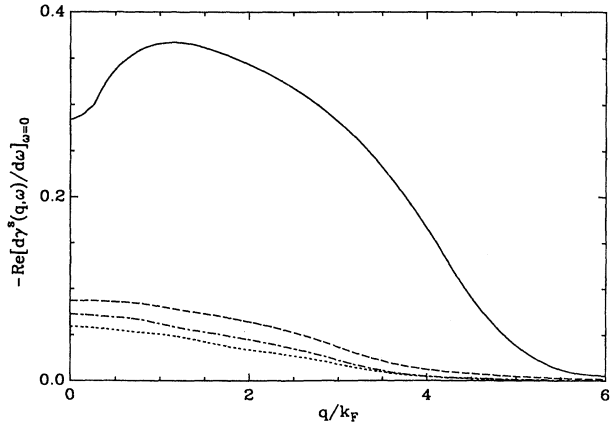

FIG. 7. $d\,\mathrm{Re}\gamma^s(\mathbf{q},\omega)/d\omega|_{\omega=0}$ for densities $r_s = 5$ (dotted line), $r_s = 10$ (dash-dotted line), $r_s = 20$ (dashed line), and $r_s = 40$ (solid line). This represents renormalization of the single particle and hole propagation.

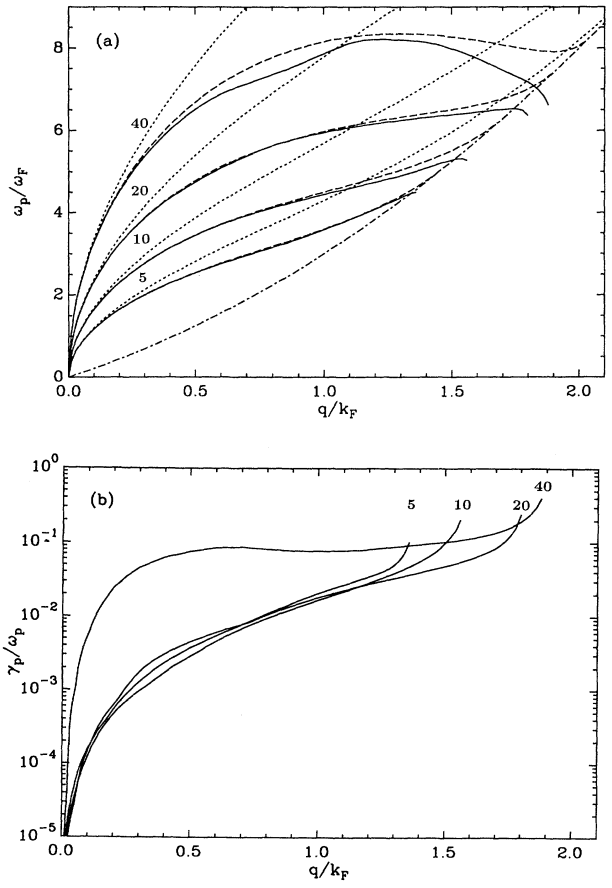

FIG. 8. (a) Plasmon dispersion curves for densities $r_s = 5$, 10, 20, and 40 (solid lines). The dashed lines show the corresponding curves when $\gamma(\mathbf{q},z)$ and $\gamma^s(\mathbf{q},z)$ are set equal to zero. The dotted lines are the RPA curves, and the dash-dotted boundary marks the edge of the single-particle excitation region for the RPA. (b) Fractional width at half-maximum $\Delta\omega(\mathbf{q})/\omega_p(\mathbf{q})$ of the plasmon resonance as a function of $\mathbf{q}$ for $r_s = 5$, 10, 20, and 40.

ever, for $r_s = 40$ the plasmon width exceeds 10% for $|\mathbf{q}|/k_F \gtrsim 0.3$. For larger $|\mathbf{q}|/k_F$ the width then remains approximately constant up to $|\mathbf{q}|/k_F \lesssim 1$. We conclude that right through to the solidification point the plasmon remains a well-defined resonance for all $\mathbf{q}$ up to q_c.

IV. CONCLUSIONS

The theory we have developed is particularly suited to the strongly interacting electron system. The dynamic functions $\gamma(\mathbf{q},\omega)$ and $\gamma^s(\mathbf{q},\omega)$ provide a measure of the relative importance of multiparticle excitations.[11] We have investigated their effect for densities down to the point at which the correlations have become so strong that Wigner crystallization occurs. For densities $r_s \gtrsim 20$ we find that both the $\gamma(\mathbf{q},\omega)$ and $\gamma^s(\mathbf{q},\omega)$ functions significantly affect the properties of the plasmon and the additional peak in $\mathrm{Im}\chi(\mathbf{q},\omega)$. While $\gamma(\mathbf{q},\omega)$ could be incorporated into a dynamic modification of the static local-field correction $G(\mathbf{q})$, the $\gamma^s(\mathbf{q},\omega)$ is primarily associated with corrections of the single-particle part of the response function $\chi^s(\mathbf{q},\omega)$. The increasing importance of $\gamma^s(\mathbf{q},\omega)$ as the Wigner transition point is approached is consistent with our physical picture that the single-particle properties of the system will be strongly affected in this region [recalling that on the solid side of the transition $\chi^s(\mathbf{q},\omega)$ should represent the response of a single-particle localized on its lattice site].

We find that the plasmon dispersion curve as a function of ω is significantly flattened compared with the RPA curve for all densities $r_s \gtrsim 5$ by the effect of the static exchange-correlation hole. Multiparticle effects further depress the curve for $r_s \gtrsim 20$ leading to a negative dispersion for large $\mathbf{q}$.

Even though the plasmon peak develops a width when multiparticle effects are included, the plasmon resonance remains well defined for all $|\mathbf{q}| \lesssim q_c$ for densities right down to $r_s \sim 40$. This means that even though the multiparticle effects become large they are never sufficiently strong on the liquid side of the Wigner phase transition to wipe out the plasmon as a well-defined resonance.

The plasmon peak occurs on the high-energy side of the single-particle excitation spectrum, merging with it at $q_c \sim k_F$. We observe a second peak on the other side of the single-particle region at around $|\mathbf{q}|/k_F \sim 2.6$. This peak indicates that for $r_s \gtrsim 20$ the system strongly favors low-energy excitations with a $\mathbf{q}$ value matching the reciprocal lattice vector of the Wigner crystal. A very large peak develops in the static susceptibility $\chi(\mathbf{q})$ at the same point. We interpret this phenomenon as a precursor of the transition to the Wigner solid.

ACKNOWLEDGMENTS

We thank Z.W. Gortel for valuable discussions. Support of a Gordon Godfrey Grant (A.S.), and from the Australian Research Grants Scheme (L.Ś.) is acknowledged.

APPENDIX A: RESPONSE FUNCTION

We define a scalar product for any two operators A and B by the relation

$$\langle B\,|\,A\rangle = \frac{1}{\beta}\int_0^\beta d\lambda \ll B^\dagger A(i\hbar\lambda) \gg, \tag{A1}$$

where $\beta = 1/k_BT$. The angular brackets on the right-hand side of the expression are the grand canonical ensemble average. The state bra and ket vectors $\langle B\,|$ and $|\,A\rangle$ are operators in a Hilbert space of operators.

It is a property of this scalar product that

$$\langle LB\,|\,A\rangle = \frac{1}{\hbar\beta} \ll [B^\dagger, A] \gg, \tag{A2}$$

where the Liouville operator L operating on any operator A gives the commutator

$$LA = \frac{1}{\hbar}[H - \mu N, A]. \tag{A3}$$

The Hamiltonian operator H can be split into kinetic and interaction parts, which for our system are given by

$$\begin{aligned} H &= H^{\mathrm{kin}} + H^{\mathrm{int}} \\ &= \sum_{\mathbf{k}} \varepsilon_{\mathbf{k}} c_{\mathbf{k}}^\dagger c_{\mathbf{k}} \\ &\quad + \frac{1}{2\Omega}\sum_{\mathbf{k},\mathbf{k}'} v_{\mathbf{q}} c_{\mathbf{k}'+\mathbf{q}/2}^\dagger c_{\mathbf{k}-\mathbf{q}/2}^\dagger c_{\mathbf{k}+\mathbf{q}/2} c_{\mathbf{k}'-\mathbf{q}/2}, \end{aligned} \tag{A4}$$

where $v_{\mathbf{q}}$ is the bare Coulomb interaction.

For future use it is convenient to also split L into kinetic and interaction parts, by defining operators L^{kin} and L^{int}:

$$\begin{aligned} L^{\mathrm{kin}}A &= \frac{1}{\hbar}[H^{\mathrm{kin}} - \mu N, A], \\ L^{\mathrm{int}}A &= \frac{1}{\hbar}[H^{\mathrm{int}}, A]. \end{aligned} \tag{A5}$$

We also note a useful relation,

$$L\rho_{\mathbf{q}} = \frac{1}{\hbar}[H - \mu N, \rho_{\mathbf{q}}] = -|\mathbf{q}|J_{\mathbf{q}}. \tag{A6}$$

where the density and longitudinal current operators are defined as

$$\begin{aligned} \rho_{\mathbf{q}} &= \sum_{\mathbf{k}} \rho_{\mathbf{q}}^{\mathbf{k}}, \\ J_{\mathbf{q}} &= \frac{\hbar}{m}\sum_{\mathbf{k}} \hat{\mathbf{q}}\cdot\mathbf{k}\,\rho_{\mathbf{q}}^{\mathbf{k}}. \end{aligned} \tag{A7}$$

With the help of Eq. (A2) we can write the generalized response function [Eq. (2)] in the scalar product form

$$\chi_{\mathbf{k}\mathbf{k}'}(\mathbf{q},t) = \frac{i\beta}{\Omega}\theta(t)\langle L\rho_{-\mathbf{q}}^{\mathbf{k}}(t)\,|\,\rho_{-\mathbf{q}}^{\mathbf{k}'}(0)\rangle. \tag{A8}$$

The Laplace transform of this can be expressed as

$$\chi_{\mathbf{k}\mathbf{k}'}(\mathbf{q},z)=\int_0^\infty dt\, e^{izt}\chi_{\mathbf{k}\mathbf{k}'}(\mathbf{q},t) \quad (\mathrm{Im}z>0)$$
$$=-\frac{\beta}{\Omega}\left\langle \rho^{\mathbf{k}}_{-\mathbf{q}}\left|\frac{L}{z-L}\right|\rho^{\mathbf{k}'}_{-\mathbf{q}}\right\rangle. \tag{A9}$$

The static generalized response function $\chi_{\mathbf{k}\mathbf{k}'}(\mathbf{q})\equiv\chi_{\mathbf{k}\mathbf{k}'}(\mathbf{q},z=0)$, and the static response function $\chi(\mathbf{q})$ are given by

$$\chi_{\mathbf{k}\mathbf{k}'}(\mathbf{q})=\frac{\beta}{\Omega}\langle\rho^{\mathbf{k}}_{-\mathbf{q}}|\rho^{\mathbf{k}'}_{-\mathbf{q}}\rangle,$$
$$\chi(\mathbf{q})=\sum_{\mathbf{k},\mathbf{k}'}\chi_{\mathbf{k}\mathbf{k}'}(\mathbf{q}). \tag{A10}$$

APPENDIX B: RELAXATION FUNCTION

The density-density relaxation function $R(\mathbf{q},t)$ describes the relaxation of the system back to its unperturbed ground state if a static external potential which has been perturbing the system is suddenly removed at $t=0$. For $t>0$ the relaxation function $R(\mathbf{q},t)$ is related to the response function of the system through

$$\chi(\mathbf{q},t)=-\chi(\mathbf{q})\frac{d}{dt}R(\mathbf{q},t). \tag{B1}$$

Comparing Eqs. (A8) and (B1) we define the generalized relaxation function $R_{\mathbf{k}\mathbf{k}'}(\mathbf{q},t)$ as

$$R_{\mathbf{k}\mathbf{k}'}(\mathbf{q},t)=\frac{\beta}{\Omega}\sum_{\mathbf{k}''}\langle\rho^{\mathbf{k}}_{-\mathbf{q}}(t)|\rho^{\mathbf{k}''}_{-\mathbf{q}}(0)\rangle\chi^{-1}_{\mathbf{k}''\mathbf{k}'}(\mathbf{q}). \tag{B2}$$

This describes the relaxation of one particular microscopic freedom labeled by $\mathbf{k}$ with the external perturbation coupled only to one degree of freedom $\mathbf{k}'$. The density-density relaxation function $R(\mathbf{q},t)$ can be recovered from $R_{\mathbf{k}\mathbf{k}'}(\mathbf{q},t)$:

$$R(\mathbf{q},t)=\frac{1}{\chi(\mathbf{q})}\sum_{\mathbf{k},\mathbf{k}',\mathbf{k}''}R_{\mathbf{k}\mathbf{k}''}(\mathbf{q},t)\chi_{\mathbf{k}''\mathbf{k}'}(\mathbf{q}). \tag{B3}$$

The Laplace transform of Eq. (B2) can be expressed as

$$R_{\mathbf{k}\mathbf{k}'}(\mathbf{q},z)=\frac{i\beta}{\Omega}\sum_{\mathbf{k}''}\left\langle\rho^{\mathbf{k}}_{-\mathbf{q}}\left|\frac{1}{z-L}\right|\rho^{\mathbf{k}''}_{-\mathbf{q}}\right\rangle\chi^{-1}_{\mathbf{k}''\mathbf{k}'}(\mathbf{q}). \tag{B4}$$

The relaxation function $R_{\mathbf{k}\mathbf{k}'}(\mathbf{q},z)$ is related to the generalized response function $\chi_{\mathbf{k}\mathbf{k}'}(\mathbf{q},z)$. Comparing Eqs. (A9) and (B4) we have

$$\chi_{\mathbf{k}\mathbf{k}'}(\mathbf{q},z)=\sum_{\mathbf{k}''}[\delta_{\mathbf{k}\mathbf{k}''}+izR_{\mathbf{k}\mathbf{k}''}(\mathbf{q},z)]\chi_{\mathbf{k}''\mathbf{k}'}(\mathbf{q}). \tag{B5}$$

APPENDIX C: KINETIC EQUATION

To evaluate the relaxation function $R_{\mathbf{k}\mathbf{k}'}(\mathbf{q},z)$, we start by introducing a projection operator P which projects the total Hilbert space of operators on to the subspace spanned by the single particle-hole operators $|\rho^{\mathbf{k}}_{-\mathbf{q}}\rangle$:

$$P=P^2=\frac{\beta}{\Omega}\sum_{\mathbf{k},\mathbf{k}'}|\rho^{\mathbf{k}}_{-\mathbf{q}}\rangle\chi^{-1}_{\mathbf{k}\mathbf{k}'}(\mathbf{q})\langle\rho^{\mathbf{k}'}_{-\mathbf{q}}|. \tag{C1}$$

The inverse of the matrix $\chi_{\mathbf{k}\mathbf{k}'}(\mathbf{q})$ appears in this definition due to the nonorthonormality of the operator basis set. The projection operator complementary to P is denoted by $Q=(1-P)$.

From the definition of the operator P we can rewrite Eq. (B4) as

$$R_{\mathbf{k}\mathbf{k}'}(\mathbf{q},z)=\frac{i\beta}{\Omega}\sum_{\mathbf{k}''}\left\langle\rho^{\mathbf{k}}_{-\mathbf{q}}\left|P\frac{1}{z-L}P\right|\rho^{\mathbf{k}''}_{-\mathbf{q}}\right\rangle\chi^{-1}_{\mathbf{k}''\mathbf{k}'}(\mathbf{q}). \tag{C2}$$

Using the operator identity[21]

$$P\frac{1}{z-L}P=\frac{1}{z-PLP-\Sigma(z)}, \tag{C3}$$

with $\Sigma(z)$ defined by

$$\Sigma(z)=PLQ\frac{1}{z-QLQ}QLP, \tag{C4}$$

we can write Eq. (C2) for the matrix $\hat{R}(\mathbf{q},z)$ as

$$\hat{R}(\mathbf{q},z)=i[z-\hat{\omega}(\mathbf{q})-\hat{M}(\mathbf{q},z)]^{-1}. \tag{C5}$$

The matrix $\hat{\omega}(\mathbf{q})$ is given by

$$\omega_{\mathbf{k}\mathbf{k}'}(\mathbf{q})=\frac{\beta}{\Omega}\sum_{\mathbf{k}''}\langle L^{\mathrm{kin}}\rho^{\mathbf{k}}_{-\mathbf{q}}|\rho^{\mathbf{k}''}_{-\mathbf{q}}\rangle\chi^{-1}_{\mathbf{k}''\mathbf{k}'}(\mathbf{q}), \tag{C6}$$

and $\hat{M}(\mathbf{q},z)$ is the memory function matrix which is defined as

$$M_{\mathbf{k}\mathbf{k}'}(\mathbf{q},z)=\frac{\beta}{\Omega}\sum_{\mathbf{k}''}\langle\rho^{\mathbf{k}}_{-\mathbf{q}}|(L^{\mathrm{int}})^\dagger+\Sigma(z)|\rho^{\mathbf{k}''}_{-\mathbf{q}}\rangle\chi^{-1}_{\mathbf{k}''\mathbf{k}'}(\mathbf{q})$$
$$\equiv\frac{\beta}{\Omega}\sum_{\mathbf{k}''}\langle\rho^{\mathbf{k}}_{-\mathbf{q}}|\Gamma(z)|\rho^{\mathbf{k}''}_{-\mathbf{q}}\rangle\chi^{-1}_{\mathbf{k}''\mathbf{k}'}(\mathbf{q}). \tag{C7}$$

Equation (C7) defines the vertex operator $\Gamma(z)$. The operator $(L^{\mathrm{int}})^\dagger$ is the conjugate to L^{int}.

With the help of the identity

$$\frac{1}{z-\hat{\omega}-\hat{M}}=\frac{1}{z-\hat{\omega}}\left(1+\hat{M}\frac{1}{z-\hat{\omega}-\hat{M}}\right) \tag{C8}$$

and $\hbar\omega_{\mathbf{k}\mathbf{k}'}(\mathbf{q})\equiv\hbar\omega^{\mathbf{k}}_{\mathbf{q}}\delta_{\mathbf{k}\mathbf{k}'}$, we can express Eq. (C5) in the form of a kinetic equation for the generalized relaxation function $R_{\mathbf{k}\mathbf{k}'}(\mathbf{q},z)$:

$$(z-\omega^{\mathbf{k}}_{\mathbf{q}})R_{\mathbf{k}\mathbf{k}'}(\mathbf{q},z)=i\delta_{\mathbf{k}\mathbf{k}'}+\sum_{\mathbf{k}''}M_{\mathbf{k}\mathbf{k}''}(\mathbf{q},z)R_{\mathbf{k}''\mathbf{k}'}(\mathbf{q},z). \tag{C9}$$

Transforming Eq. (C9) back to the time domain, we obtain the familiar Langevin-type equation

$$i\frac{d}{dt}R_{\mathbf{kk}'}(\mathbf{q},t)=\frac{\hbar}{m}\mathbf{q}\cdot\mathbf{k}R_{\mathbf{kk}'}(\mathbf{q},t)+\sum_{\mathbf{k}''}\int_0^t dt'\,M_{\mathbf{kk}''}(\mathbf{q},t-t')R_{\mathbf{k}''\mathbf{k}'}(\mathbf{q},t'). \tag{C10}$$

From the definition of the memory function, Eq. (C7), it can be easily established that $M_{\mathbf{kk}'}(\mathbf{q},t)$ must satisfy the constraint $\sum_{\mathbf{k}}M_{\mathbf{kk}'}(\mathbf{q},t)=0$ [Eq. (4)]. This is related to the Ward identity. Using this equation together with the definitions of $\rho_{\mathbf{q}}$, $J_{\mathbf{q}}$, and $R_{\mathbf{kk}'}(\mathbf{q},t)$, we obtain after summing Eq. (C10) over the index $\mathbf{k}$,

$$i\frac{d}{dt}\langle\rho_{-\mathbf{q}}(t)\,|\,\rho^{\mathbf{k}'}_{-\mathbf{q}}(0)\rangle=-|\mathbf{q}|\;\langle J_{-\mathbf{q}}(t)\,|\,\rho^{\mathbf{k}'}_{-\mathbf{q}}(0)\rangle. \tag{C11}$$

This is true for all $\mathbf{k}'$, and confirms that the continuity equation is exactly satisfied.

APPENDIX D: COLLECTIVE MEMORY FUNCTION

We assume that the collective part of the memory function $M^c_{\mathbf{kk}'}(\mathbf{q},z)$ couples only to the density and current fluctations $|\,\rho_{-\mathbf{q}}\rangle$ and $|\,J_{-\mathbf{q}}\rangle$, and so we may express the collective vertex operator $\Gamma^c(z)$ in the form

$$\begin{aligned}\Gamma^c(z)=&\,|\rho_{-\mathbf{q}}\rangle M^c_{\rho\rho}(\mathbf{q},z)\langle\rho_{-\mathbf{q}}|\\&+|\rho_{-\mathbf{q}}\rangle M^c_{\rho J}(\mathbf{q},z)\langle J_{-\mathbf{q}}|\\&+|J_{-\mathbf{q}}\rangle M^c_{J\rho}(\mathbf{q},z)\langle\rho_{-\mathbf{q}}|\\&+|J_{-\mathbf{q}}\rangle M^c_{JJ}(\mathbf{q},z)\langle J_{-\mathbf{q}}|.\end{aligned} \tag{D1}$$

In this general form we have the four functions, $M^c_{\rho\rho}(\mathbf{q},z)$, $M^c_{\rho J}(\mathbf{q},z)$, $M^c_{J\rho}(\mathbf{q},z)$, and $M^c_{JJ}(\mathbf{q},z)$ that have to be specified. They are independent of the matrix labels $\mathbf{k}$ and $\mathbf{k}'$.

Equation (4) cannot be satisfied if either $M^c_{\rho\rho}(\mathbf{q},z)$ or $M^c_{\rho J}(\mathbf{q},z)$ are nonzero, and this permits us to eliminate these two functions.

$M^c_{J\rho}(\mathbf{q},z)$ has to be a static function which is independent of z. This follows from the definition of $\Sigma(z)$—which requires that $\Sigma(z)\,|\,\rho^{\mathbf{k}}_{-\mathbf{q}}\rangle=0$—and from the definitions of the operators L and P which imply that

$$\begin{aligned}QLP\,|\rho_{-\mathbf{q}}\rangle&=-|\mathbf{q}|Q\,|J_{-\mathbf{q}}\rangle\\&=\frac{\hbar}{m}\sum_{\mathbf{k}}\mathbf{q}\cdot\mathbf{k}\,Q\,|\rho^{\mathbf{k}}_{-\mathbf{q}}\rangle=0.\end{aligned} \tag{D2}$$

Equation (C7) then implies that $M^c_{J\rho}(\mathbf{q},z)$ cannot depend on z.

To write down the matrix elements of $M^c_{JJ}(\mathbf{q},z)$ and $M^c_{J\rho}(\mathbf{q})$ we need the following relations which are obtained using Eqs. (A2) and (A10),

$$\frac{\beta|\mathbf{q}|}{\Omega}\sum_{\mathbf{k}''}\langle J_{-\mathbf{q}}\,|\,\rho^{\mathbf{k}''}_{-\mathbf{q}}\rangle\chi^{-1}_{\mathbf{k}''\mathbf{k}'}(\mathbf{q})=-\frac{\beta}{\Omega}\sum_{\mathbf{k},\mathbf{k}''}\omega^{\mathbf{k}}_{\mathbf{q}}\langle\rho^{\mathbf{k}}_{-\mathbf{q}}\,|\,\rho^{\mathbf{k}''}_{-\mathbf{q}}\rangle\chi^{-1}_{\mathbf{k}''\mathbf{k}'}(\mathbf{q})=-\omega^{\mathbf{k}'}_{\mathbf{q}},$$

$$\frac{\beta}{\Omega}\sum_{\mathbf{k}''}\langle\rho_{-\mathbf{q}}\,|\,\rho^{\mathbf{k}''}_{-\mathbf{q}}\rangle\chi^{-1}_{\mathbf{k}''\mathbf{k}'}(\mathbf{q})=1, \tag{D3}$$

$$\langle\rho^{\mathbf{k}}_{-\mathbf{q}}\,|\,J_{-\mathbf{q}}\rangle=\frac{n^{\mathbf{k}}_{\mathbf{q}}}{\hbar\beta|\mathbf{q}|}.$$

Using these relations, the matrix elements of the collective part of the memory function can be reduced to the expression

$$M^c_{\mathbf{kk}'}(\mathbf{q},z)=\frac{n^{\mathbf{k}}_{\mathbf{q}}}{\hbar\beta|\mathbf{q}|}\left(M^c_{J\rho}(\mathbf{q})-M^c_{JJ}(\mathbf{q},z)\frac{\omega^{\mathbf{k}'}_{\mathbf{q}}}{|\mathbf{q}|}\right). \tag{D4}$$

APPENDIX E: STATIC EFFECTIVE INTERACTION

In this section we relate current-density memory function $M^c_{J\rho}(\mathbf{q})$ the instantaneous effective interaction between electrons $v^{\mathrm{eff}}_{\mathbf{q}}$. A direct way of making this identification is to start by setting all the other contributions to the memory function, $\gamma^s(\mathbf{q},z)$ and $M^c_{JJ}(\mathbf{q},z)$, to zero [see Eqs. (8) and (9)]. Then Eq. (5) can be rewritten with the help of Eq. (B5) as an equation for $\chi_{\mathbf{kk}'}(\mathbf{q},z)$,

$$(z-\omega^{\mathbf{k}}_{\mathbf{q}})\chi_{\mathbf{kk}'}(\mathbf{q},z)=\frac{n^{\mathbf{k}}_{\mathbf{q}}}{\hbar\Omega}\left(\delta_{\mathbf{kk}'}+\frac{\Omega}{\beta|\mathbf{q}|}M^c_{J\rho}(\mathbf{q})\sum_{\mathbf{k}''}\chi_{\mathbf{k}''\mathbf{k}'}(\mathbf{q},z)\right). \tag{E1}$$

Dividing this by $(z-\omega^{\mathbf{k}}_{\mathbf{q}})$ and summing over $\mathbf{k}$ and $\mathbf{k}'$ we obtain the response function

$$\begin{aligned}\chi(\mathbf{q},z)&=\chi^0(\mathbf{q},z)+\chi^0(\mathbf{q},z)\frac{\Omega}{\beta|\mathbf{q}|}M^c_{J\rho}(\mathbf{q})\chi(\mathbf{q},z)\\&=\frac{\chi^0(\mathbf{q},z)}{1-\dfrac{\Omega}{\beta|\mathbf{q}|}M^c_{J\rho}(\mathbf{q})\chi^0(\mathbf{q},z)},\end{aligned} \tag{E2}$$

where

$$\chi^0(\mathbf{q},z)=\frac{1}{\hbar\Omega}\sum_{\mathbf{k}}\frac{n^{\mathbf{k}}_{\mathbf{q}}}{z-\omega^{\mathbf{k}}_{\mathbf{q}}} \tag{E3}$$

is the free-electron response function.[3]

The memory function $M^c_{J\rho}(\mathbf{q})$ plays the role in Eq. (E2) of a static effective potential which we can write in the form

$$v^{\mathrm{eff}}_{\mathbf{q}}\equiv-\frac{\Omega}{\beta|\mathbf{q}|}M^c_{J\rho}(\mathbf{q})=v_{\mathbf{q}}\,[1-G(\mathbf{q})], \tag{E4}$$

thus recovering the local-field construction introduced by Hubbard.[1] $v^{\mathrm{eff}}_{\mathbf{q}}$ takes account of the instantaneous exchange and correlations between an electron and its surroundings.

APPENDIX F: CURRENT-CURRENT MEMORY FUNCTION

In this section we relate the functions $M^c_{JJ}(\mathbf{q},z)$, $\gamma(\mathbf{q},z)$, and $\gamma^s(\mathbf{q},z)$ [see Eq. (11)]. In Sec. II we split the memory function $M_{\mathbf{kk}'}(\mathbf{q},z)$ into two parts

$$M_{\mathbf{kk}'}(\mathbf{q},z) = M^s_{\mathbf{kk}'}(\mathbf{q},z) + M^c_{\mathbf{kk}'}(\mathbf{q},z). \tag{F1}$$

We define $\gamma(\mathbf{q},z)$ as the current-current expectation value of the full memory function:

$$\gamma(\mathbf{q},z) = \frac{m\beta}{n\Omega}\langle J_{-q}\,|\,\Gamma(z)\,|\,J_{-q}\rangle, \tag{F2}$$

where $\Gamma(z)$ is the vertex operator defined in Eq. (C7). If we multiply both sides of Eq. (F1) by $\omega^{\mathbf{k}}_{\mathbf{q}} n^{\mathbf{k}'}_{\mathbf{q}}$ and sum over $\mathbf{k}$ and $\mathbf{k}'$ we can project the equation on to the current basis. Then using Eqs. (8), (9), and (C7) we get

$$\gamma(\mathbf{q},z) = \gamma^s(\mathbf{q},z) + \frac{\Omega n}{\beta m} M^c_{JJ}(\mathbf{q},z)\ , \tag{F3}$$

which is Eq. (11).

Direct calculation using time reversal symmetry shows that $\langle J_{-q}\,|\,(L^{\rm int})^\dagger\,|\,J_{-q}\rangle$ vanishes. From our expression for $\Sigma(z)$ [Eq. (C4)] we may therefore write

$$\gamma(\mathbf{q},z) = \frac{m\beta}{n\Omega}\left\langle LJ_{-q}\left|Q\frac{1}{z-QLQ}Q\right|LJ_{-q}\right\rangle. \tag{F4}$$

Evaluating the commutator $LJ_{-q} = \hbar^{-1}[H, J_{-q}]$ [Eq. (A3)], and using the property of the Q projection operator that $Q\,|\,LJ_{-q}\rangle = Q\,|\,L^{\rm int}J_{-q}\rangle$, we obtain

$$\gamma(\mathbf{q},z) = \frac{\beta}{nm\Omega^3}\sum_{\mathbf{q}',\mathbf{q}''} v_{\mathbf{q}'}(\hat{\mathbf{q}}\cdot\mathbf{q}')\left\langle \rho_{\mathbf{q}'-\mathbf{q}}\rho_{-\mathbf{q}'}\left|\frac{Q}{z-QLQ}\right|\rho_{\mathbf{q}''-\mathbf{q}}\rho_{-\mathbf{q}''}\right\rangle(\hat{\mathbf{q}}\cdot\mathbf{q}'')v_{\mathbf{q}''}. \tag{F5}$$

By introducing the fluctuation-dissipation theorem, in the zero-temperature limit Eq. (F5) can be cast in the form

$$\begin{aligned}
\gamma(\mathbf{q},z) &= \int_{-\infty}^{\infty}\frac{d\omega}{2\pi}\frac{1}{\omega(z-\omega)}\int_{-\infty}^{\infty} dt\, e^{i\omega t}\bar{\gamma}(\mathbf{q},t), \\
\bar{\gamma}(\mathbf{q},t) &= \frac{1}{\hbar nm\Omega^3}\sum_{\mathbf{q}',\mathbf{q}''} v_{\mathbf{q}'}(\hat{\mathbf{q}}\cdot\mathbf{q}') \ll \rho_{\mathbf{q}'}\rho_{\mathbf{q}-\mathbf{q}'}Q\mathrm{e}^{-iQLQ\cdot t}\rho_{\mathbf{q}''-\mathbf{q}}\rho_{-\mathbf{q}''}\gg(\hat{\mathbf{q}}\cdot\mathbf{q}'')v_{\mathbf{q}''} \\
&= -\frac{1}{\hbar nm\Omega}\int d\mathbf{r}_1 d\mathbf{r}_1' d\mathbf{r}_2 d\mathbf{r}_2' \mathrm{e}^{i\mathbf{q}\cdot(\mathbf{r}_1-\mathbf{r}_1')}[(\hat{\mathbf{q}}\cdot\nabla_{\mathbf{r}_1'})v(\mathbf{r}_1'-\mathbf{r}_2')] \\
&\quad\times[\ll\rho(\mathbf{r}_2')\rho(\mathbf{r}_1')Q\mathrm{e}^{-iQLQt}\rho(\mathbf{r}_1)\rho(\mathbf{r}_2)\gg][(\hat{\mathbf{q}}\cdot\nabla_{\mathbf{r}_2'})v(\mathbf{r}_2-\mathbf{r}_1)].
\end{aligned} \tag{F6}$$

The four-point density expectation value in Eq. (F6) gives the probability of finding two density fluctuations at time $t=0$ at positions $\mathbf{r}_1$ and $\mathbf{r}_2$, which then propagate to positions $\mathbf{r}_1$ and $\mathbf{r}_2$ at the later time t. We approximately factorize it into products of two-point density expectation values,

$$\begin{aligned}
\ll\rho(\mathbf{r}_2')\rho(\mathbf{r}_1')Q\mathrm{e}^{-iQLQt}\rho(\mathbf{r}_1)\rho(\mathbf{r}_2)\gg &= g(\mathbf{r}_1'-\mathbf{r}_2')[\ll\delta\rho(\mathbf{r}_1',t)\delta\rho(\mathbf{r}_1,0)\gg\ll\delta\rho(\mathbf{r}_2',t)\delta\rho(\mathbf{r}_2,0)\gg \\
&\quad+\ll\delta\rho(\mathbf{r}_1',t)\delta\rho(\mathbf{r}_2,0)\gg\ll\delta\rho(\mathbf{r}_2',t)\delta\rho(\mathbf{r}_1,0)\gg]g(\mathbf{r}_1-\mathbf{r}_2),
\end{aligned} \tag{F7}$$

where $\delta\rho(\mathbf{r},t) = \rho(\mathbf{r},t) - n$. Equation (F7) describes the independent propagation of two density fluctuations, the first from $\mathbf{r}_1$ to $\mathbf{r}_1'$ and the second from $\mathbf{r}_2$ to $\mathbf{r}_2'$. The static density-density correlation functions $g(\mathbf{r}_1'-\mathbf{r}_2')$ and $g(\mathbf{r}_1-\mathbf{r}_2)$ correlate the two fluctuations at their starting and finishing points. This simulates the interaction of the first density fluctuation with its surrounding exchange-correlation hole. The presence of the operator Q which projects out excitations involving a single density fluctuation means that the lowest-order Hartree-Fock-type terms in which one of the pair of flucuations is averaged over cannot contribute in Eq. (F7).

Equation (13) follows from Eqs. (F6) and (F7) by recalling the definition of the van Hove density-density correlation function, $S(\mathbf{r},t;\mathbf{r}',t') \equiv \ll\delta\rho(\mathbf{r},t)\delta\rho(\mathbf{r}',t')\gg$.

Turning now to $\gamma^s(\mathbf{q},z)$, this describes the coupling of the single-particle part of the density fluctuation with its surroundings, and by analogy with Eq. (F7) we postulate

$$\begin{aligned}
\gamma^s(\mathbf{q},z) &= \int_{-\infty}^{\infty}\frac{d\omega}{2\pi}\frac{1}{\omega(z-\omega)}\int_{-\infty}^{\infty} dt\, e^{i\omega t}\bar{\gamma}^s(\mathbf{q},t), \\
\bar{\gamma}^s(\mathbf{q},t) &= -\frac{1}{\hbar nm\Omega}\int dr_1 dr_1' dr_2 dr_2'\, \mathrm{e}^{i\mathbf{q}\cdot(\mathbf{r}_1-r_1')}[(\hat{\mathbf{q}}\cdot\nabla_{\mathbf{r}_1'})v(\mathbf{r}_1'-\mathbf{r}_2')] \\
&\quad\times g(\mathbf{r}_1'-\mathbf{r}_2')[\ll\delta\rho(\mathbf{r}_1',t)\delta\rho(\mathbf{r}_1)\gg^{\rm s}\ll\delta\rho(\mathbf{r}_2',t)\delta\rho(\mathbf{r}_2)\gg]g(\mathbf{r}_1'-\mathbf{r}_2')[(\hat{\mathbf{q}}\cdot\nabla_{\mathbf{r}_2'})v(\mathbf{r}_2-\mathbf{r}_1)],
\end{aligned} \tag{F8}$$

where $\ll\delta\rho(\mathbf{r}_1',t)\delta\rho(\mathbf{r}_1)\gg^{\rm s}$ is a density fluctuation from which the collective component has been projected out. It is uniquely specified through the fluctuation-dissipation theorem by $R^s_{\mathbf{kk}'}(\mathbf{q},z)$. We obtain Eq. (14) from Eq. (F8) by introducing the corresponding single-particle density-density correlation function $S^{\rm s}(\mathbf{r},t;\mathbf{r}',t') \equiv \ll\delta\rho(\mathbf{r},t)\delta\rho(\mathbf{r}',t')\gg^{\rm s}$.

*Permanent address: Institute of Physics, Polish Academy of Sciences, Al. Lotników 32/46, PL-02-668 Warszawa, Poland.

[1] J. Hubbard, Proc. R. Soc. London Ser. A **243**, 336 (1957).
[2] K. S. Singwi and M. P. Tosi, in *Solid State Physics*, edited by H. Ehrenreich, F. Seitz, and D. Turnbull (Academic, New York, 1981), Vol. 36, p. 177.
[3] J. Lindhard, K. Dan. Vidensk. Selsk. Mat.-Fys. Medd. **28** (8), 1 (1954) for three-dimensional system; F. Stern, Phys. Rev. Lett. **18**, 546 (1967) for two-dimensional system.
[4] K. S. Singwi, M. P. Tosi, R. H. Land, and A. Sjölander, Phys. Rev. **176**, 589 (1968).
[5] D. N. Lowy and G. E. Brown, Phys. Rev. B **12**, 2138 (1975).
[6] K. S. Bedell and G. E. Brown, Phys. Rev. B **17**, 4512 (1978).
[7] D. M. Ceperley and B. Adler, Phys. Rev. Lett. **45**, 566 (1980).
[8] B. Goodman and A. Sjölander, Phys. Rev. B **8**, 200 (1973).
[9] N. Iwamoto, E. Krotschek, and D. Pines, Phys. Rev. B **29**, 3936 (1984).
[10] F. Green, D. Neilson, and J. Szymański, Phys. Rev. B **31**, 2779 (1985); **31**, 2796 (1985); **31**, 5837 (1985).
[11] F. Green, D. Neilson, D. Pines, and J. Szymański, Phys. Rev. B **35**, 133 (1987).
[12] H. Mori, Prog. Theor. Phys. **33**, 423 (1965).
[13] J. P. Boon and S. Yip, *Molecular Hydrodynamics* (McGraw-Hill, New York, 1980).
[14] C. D. Boley and J. H. Smith, Phys. Rev. A **12**, 661 (1975); Phys. Rev. B **17**, 4260 (1978).
[15] O. T. Valls, G. F. Mazenko, and H. Gould, Phys. Rev. B **18**, 263 (1978); O. T. Valls, H. Gould, and G. F. Mazenko, *ibid.* **25**, 1663 (1982).
[16] W. Götze, J. Phys. C **12**, 1279 (1979); Philos. Mag. **43**, 219 (1981).
[17] J. P. Boon and S. Yip, *Molecular Hydrodynamics* (McGraw-Hill, New York, 1980).
[18] B. Tanatar and D. M. Ceperley, Phys. Rev. B **39**, 5005 (1989).
[19] A. Czachor, A. Holas, S. R. Sharma, and K. S. Singwi, Phys. Rev. B **29**, 2144 (1982).
[20] A. Holas and K. S. Singwi, Phys. Rev. B **40**, 158 (1989).
[21] A. Messiah, *Quantum Mechanics* (North-Holland, Amsterdam, 1961).